THE PROLONGED GASTROINTESTINAL SYNDROME IN RHESUS MACAQUES: THE RELATIONSHIP BETWEEN GASTROINTESTINAL, HEMATOPOIETIC, AND DELAYED MULTI-ORGAN SEQUELAE FOLLOWING ACUTE, POTENTIALLY LETHAL, PARTIAL-BODY IRRADIATION

Thomas J. MacVittie[*], **Alexander Bennett**[*], **Catherine Booth**[†], **Michael Garofalo**[*], **Gregory Tudor**[†], **Amanda Ward**[*], **Terez Shea-Donohue**[‡], **Daniel Gelfond**[§], **Emylee McFarland**[**], **William Jackson III**[††], **Wei Lu**[‡‡], and **Ann M. Farese**[*]

[*]University of Maryland, School of Medicine, Department of Radiation Oncology

[†]Epistem Ltd, Manchester, UK

[‡]University of Maryland, School of Medicine, Mucosal Biology Research Center

[§]Digestive Diseases and Nutrition Center, Women and Children's Hospital of Buffalo

[**]U.S. Army Medical Research Institute of Chemical Defense, Oak Ridge Institute for Science and Education

[††]Statistician, Rockville, MD

[‡‡]University of Maryland Medical Center, Department of Radiation Oncology

Abstract

The dose response relationship for the acute gastrointestinal syndrome following total-body irradiation prevents analysis of the full recovery and damage to the gastrointestinal system, since all animals succumb to the subsequent 100% lethal hematopoietic syndrome. A partial-body irradiation model with 5% bone marrow sparing was established to investigate the prolonged effects of high-dose radiation on the gastrointestinal system, as well as the concomitant hematopoietic syndrome and other multi-organ injury including the lung. Herein, cellular and clinical parameters link acute and delayed coincident sequelae to radiation dose and time course post-exposure. Male rhesus *Macaca mulatta* were exposed to partial-body irradiation with 5% bone marrow (tibiae, ankles, feet) sparing using 6 MV linear accelerator photons at a dose rate of 0.80 Gy min^{-1} to midline tissue (thorax) doses in the exposure range of 9.0 to 12.5 Gy. Following irradiation, all animals were monitored for multiple organ-specific parameters for 180 d. Animals were administered medical management including administration of intravenous fluids, antiemetics, prophylactic antibiotics, blood transfusions, antidiarrheals, supplemental nutrition,

and analgesics. The primary endpoint was survival at 15, 60, or 180 d post-exposure. Secondary endpoints included evaluation of dehydration, diarrhea, hematologic parameters, respiratory distress, histology of small and large intestine, lung radiographs, and mean survival time of decedents. Dose- and time-dependent mortality defined several organ-specific sequelae, with LD50/15 of 11.95 Gy, LD50/60 of 11.01 Gy, and LD50/180 of 9.73 Gy for respective acute gastrointestinal, combined hematopoietic and gastrointestinal, and multi-organ delayed injury to include the lung. This model allows analysis of concomitant multi-organ sequelae, thus providing a link between acute and delayed radiation effects. Specific and multi-organ medical countermeasures can be assessed for efficacy and interaction during the concomitant evolution of acute and delayed key organ-specific subsyndromes.

INTRODUCTION

THE MAJOR organ sequelae consequent to high-dose radiation exposure are the hematopoietic (H) and acute gastrointestinal (GI) acute radiation subsyndromes (ARS), followed by the delayed effects of acute radiation exposure (DEARE) characterized by multi-organ injury to include pulmonary damage. Each of these sequelae may be associated with high morbidity and mortality. Therefore, mitigating the adverse health effects of acute, high-dose radiation will require refined animal models and new treatment paradigms. The consortium, Medical Countermeasures Against Radiological Threats (MCART), established a research platform focused on development of well characterized animal models to assess medical countermeasure (MCM) efficacy against the ARS and DEARE. This research platform elucidated knowledge gaps relative to the treatment of the key organ sequelae in the context of a nuclear terrorist or accidental exposure to potentially lethal doses of radiation. These were: a) total-body irradiation (TBI) or whole thorax lung irradiation (WTLI) models provide the requisite dose- and time-dependent relationships for the hematopoietic (H)- and gastrointestinal (GI)-ARS and delayed lung damage but prevent the analysis of the full extent of damage and long-term recovery for the coincident H and GI systems to include the initiation and progression of lung and other multi-organ injury in a nuclear exposure scenario; b) there are no models that permit concurrent analysis of coincident short- and long-term damage to the GI, H, lung and other organ systems in a dose- and time-dependent manner; and c) there are no models that permit analysis of MCM effects across organ systems to establish the efficacy or potential negative interaction of a polypharmacy approach to enhance survival and overall quality of life.

The radiation exposure consequent to a nuclear terrorist or accident event will be ill-defined as a result of body position, random shielding, differential dose rate, distance from the source, and radiation intensity in the immediate or short-term fallout field. These factors predict a non-uniform and heterogeneous exposure to all victims. Additionally, the interval between exposure and treatment will be less than optimal. The optimistic aspect for those victims exposed to potentially lethal doses of radiation is that the dose distribution to the

body will be highly variable with the sparing of organ-specific stem and progenitor cells within their respective niche. This tissue-sparing effect will enhance the potential for spontaneous recovery as well as the efficacy of MCM.

The non-human primate (NHP) model described herein utilizes bilateral, uniform radiation exposure to 95% of the body to midline tissue dose (MLTD) without exposure of tibiae, ankles and feet, resulting in an approximate 5% bone marrow (BM) sparing (Taketa et al. 1970). This model permits analysis of the acute GI-ARS and the coincident H-ARS with concomitant GI damage, prolonged GI damage, and initiation and expression of delayed effects characterized by multi-organ injury including the lung, as well as the linkage among the sub-syndromes (Fig. 1). The model recognizes that the ARS and DEARE are composites of dose- and time-dependent organ-specific damage. A comparative 2-parameter analysis is provided, focused on the lethal dose response relationships (DRR) and the respective slopes of the major subsyndromes of the ARS and DEARE.

MATERIALS AND METHODS

Animals

Male rhesus macaques ($n = 81$), *Macaca mulatta*, [5.5–11.3 kg body weight (bw)] were exposed to bilateral partial-body irradiation sparing the tibiae, ankles, and feet (PBI/BM5) to doses from 9.0 and 12.5 Gy. Sixty-four animals established the respective DRR across the three major time- and dose-dependent sequelae. These animals were observed for up to 180 d post-irradiation, or until they were euthanized as per the criteria detailed below. Additional animals ($n = 16$) were irradiated to 10.0 Gy and euthanized at predetermined time points to collect tissue for histological analysis of crypt and villus damage. The time points included days 7 ($n = 2$), 34 ($n = 3$), 44 ($n = 3$), 62 ($n = 4$), 100 ($n = 3$), and 119 ($n = 1$). One (1) additional animal was irradiated to 12.0 Gy and euthanized in the same manner at day 29 but was not used for histological analysis. When applicable, these animals were also included in the DRR analysis of mortality and morbidity at the 15- and 60-d time points.

All NHPs enrolled in the study were in good health; sero-negative for simian immunodeficiency virus, simian T-cell leukemia virus type 1, and malaria; and negative for herpes B virus and tuberculosis. A pool of donor NHPs (bw 7 kg) was used for blood donation. Animals were acclimated to a supine restraint device prior to irradiation. All animal procedures were performed according to an approved Institutional Animal Care and Use Committee (IACUC) protocol.

Housing, care, food, and water—Animal housing and care were performed in accordance with the Animal Welfare Act (7 U.S.C. 2131 et. seq.) and the *Guide for the Care and Use of Laboratory Animals*. Irradiated animals were single-housed in stainless steel cages at the University of Maryland Association for Assessment and Accreditation of Laboratory Animal Care (AAALAC)-accredited animal facility. Animals were provided certified primate chow ad libitum that was supplemented with fresh fruit (i.e., apples, bananas, oranges) and primate treats. Following irradiation, citrus was eliminated from their diet. The animals had unlimited access to water that had been deionized, filtered through carbon and sand, and disinfected with UV light.

Anesthesia—Ketamine (Ketaset, 800 5th St., NW, Fort Dodge, IA 50501) (10 ± 5 mg kg^{-1}), either alone or in combination with xylazine (AnaSed, Fort Dodge, IA) (1 ± 0.5 mg kg^{-1}), was administered intramuscularly (IM) to sedate animals prior to procedures. Yohimbine (Yobine, Lloyd, Inc., 604West Thomas Ave., Shenandoah, IA 51601 USA) [(0.2 ± 0.1 mg kg^{-1}, IM or intravenously (IV)] was administered to reverse xylazine sedation, if required.

Radiation exposure and dosimetry

Approximately 18 h prior to exposure, food was removed from each animal's cage to minimize the occurrence of radiation-induced emesis. On the day of irradiation, NHPs were administered an antiemetic, Zofran (Glaxo-SmithKline, 5 Moore Dr., Research Triangle Park, Durham, NC 27713 USA) or Ondansetron, (Hospira, Inc., 275 North Field Dr., Lake Forest, IL 60045 USA) ($1-2$ mg kg^{-1} IV or IM), 45–90 min prior to exposure. Anesthetized NHPs were placed in a Plexiglas supine restraint device, and then transported from the NHP housing area to the linear accelerator (LINAC) facility at the University of Maryland, Department of Radiation Oncology.

The NHPs were administered xylazine to ensure proper radiation field placement would be maintained and then exposed to PBI/BM5 with 6MV LINAC-derived photons. PBI was delivered at an approximate dose rate of 0.80 Gy min^{-1}. The MLTD doses delivered included 9.0 Gy, 10.0 Gy, 11.0 Gy, 11.5 Gy, 12.0 Gy, and 12.5 Gy. Animals were positioned such that their tibiae were outside of the beam field. Animals were observed via in-room cameras throughout the exposure procedure. Following PBI, NHPs were anesthetized, transported back to the NHP housing area, administered Lactated Ringer's Solution (LRS) ($10-15$ mL kg^{-1} IV) and a second dose of Zofran or Ondansetron ($1-2$ mg kg^{-1} IM or IV), and returned to their home cage.

Prior to beginning the study, the LINAC was calibrated in the geometry used for NHP irradiation. Depth dose measurements were made at the center of a cylindrical phantom that approximates the mean diameter of the experimental rhesus macaque. Three phantoms of increasing size were available. The phantom is made of 0.32-cm Lucite and filled with water. Dose measurements were performed with ion chambers. Absorbed dose to water per unit machine monitor unit (MU) was obtained. The calibration was then transferred to a constancy system for daily quality assurance purposes.

During NHP irradiations, in vivo dosimetry was performed using a silicon diode system. One diode was placed on the chest to measure the delivered dose, and another was secured on the tibiae to confirm that the tissue outside of the beam field was spared irradiation. Quality assurance and control procedures that were performed prior to each set of NHP irradiations included LINAC energy output checks and diode calibrations.

Medical management

Cage side observations—Non-sedated NHPs were observed at a minimum twice daily by trained staff. Activity, posture, stool consistency, presence of blood in stool, emesis, hemorrhage, respiratory activity, seizure activity, and alopecia were graded and recorded.

Clinical observations—NHPs were anesthetized daily from day 0–21 to assess clinical parameters such as bw, body temperature, hydration status, presence of mouth ulcers, and a complete blood count (CBC) (Beckman Coulter Ac·T diff, Beckman Coulter, Inc., 11800 SW 147th Ave., Miami, FL 33196 USA) including a manual white blood cell (WBC) differential performed on a Wright-Giemsastained blood film. After day 21, clinical observations and supportive measures were performed weekly through day 60 and biweekly thereafter unless the animal's health status required more frequent intervention.

Analgesics—Buprenorphine HCl (Hospira, Lake Forest, IL) [(0.01 mg kg^{-1} to 0.02 mg kg^{-1} IM twice a day (BID)] was administered from 5 to 35 d post-irradiation and when mouth ulcers or bloody stool were observed. Doses were increased for mouth ulcers and bloody stool. Mouth ulcers were cleansed with hydrogen peroxide or Nolvasan solution and rinsed with saline. Bupivacaine gel, a mixture of 0.1 mL of 25% Bupivacaine HCl (Marcaine, Hospira) with a dab of surgical lubricant (Surgilube, Fougera, 60 Baylis Rd., Melville, NY 11747) was applied to the area with a cotton-tipped applicator.

Antiemetic—Zofran [(0.1–0.2 mg kg^{-1} IV or IM, once a day (QD) or BID] was administered when evidence of emesis was observed.

Antiulcerative—Sucralfate (Carafate, Axcan Scandipharm Inc., 22 Inverness Center Pkwy., Birmingham, AL 35242 USA; Nostrum Laboratories, Inc., 11D Jules Lane, New Brunswick, NJ 08901 USA) was administered [0.5 g by mouth (PO) or by oral gavage (OG) BID] from 5 to 35 d post-irradiation and when mouth ulcers or bloody stool were observed.

Antidiarrheals—Antidiarrheal treatment was administered according to a three-tier system of grading stool consistency, where grade 0 indicated formed stool, grade 1 indicated soft stool, and grade 2 indicated diarrhea. Following the observation of diarrhea, Loperamide Hydrochloride (Imodium, McNeil Consumer Healthcare, 7050 Camp Hill Rd., Fort Washington, PA19031USA) (0.1–0.2mgkg^{-1}PO or by OG BID) was administered. If diarrhea persisted after three successive days of Imodium treatment, or if watery stool was observed, diphenoxylate hydrochloride (Lomotil, Pfizer Inc, 235 East 42nd St., New York, NY 10017 USA) (0.1 mg kg^{-1} PO or by OG BID) was administered. If diarrhea persisted after three successive days of Lomotil treatment, Imodium treatment was repeated. If diarrhea persisted after another three successive days of Imodium treatment, Lomotil treatment was repeated. Antidiarrheal treatment was discontinued upon observation of formed stool.

Antibiotics—Antibiotics were initiated when the absolute neutrophil count (ANC) was <500 μL^{-1} and continued until the animal maintained an ANC >500 μL^{-1} for 48 h. The primary antibiotic administered was enrofloxacin (Baytril, Bayer HealthCare LLC, 12809 Shawnee Mission Pkwy., Shawnee Mission, KS 66216 USA) (10 mg kg^{-1} IM or IV, QD). Additionally, gentamicin sulfate (GentaMax, Phoenix Pharmaceutical, Inc., 1302 South 59th St., St. Joseph, MO 64507 USA) (5 mg kg^{-1} IM or IV, QD) was administered in combination with Baytril when the body temperature was 103.0°F and was continued for 24 to 48 h. Rocephin (Roche Laboratories Inc., 340 Kingsland St., Nutley, NJ 07110 USA) (50 mg kg^{-1} IM, QD) or Primaxin (Merck & Co Inc., 1 Merck Dr., Whitehouse Station, NJ

08889 USA) (10 mg kg^{-1} IM, BID) was administered when microbial resistance was demonstrated to enrofloxacin or gentamicin via positive blood culture sensitivity results or persistent fever.

Antiinflammatory (corticosteroids)—Dexamethasone (Butler Schein Animals Health, 400 Metro Place N #100, Dublin, OH 43017 USA) was administered to animals noted to be in respiratory distress [>80 breaths per min (bpm)] during daily cageside observations. The dose, frequency, and duration of treatment were at the discretion of the consulting veterinarian. Generally, NHPs were treated with a planned taper as follows: 1 mg kg^{-1} IM, BID on the first day of treatment; 0.5 mg kg^{-1} BID for 3 d; 0.5 mg kg^{-1} QD for 3 d; and 0.5 mg kg^{-1} every other day (QOD) for three doses.

Antipyretic—Carprofen(Rimadyl,Pfizer Inc.) (2.2mgkg^{-1} BID or 4.4 mg kg^{-1} IM or IV, QD) was administered when a body temperature 104.0°F was observed. It was continued for 48 h after the first day the temperature was <104.0°F.

Diuretic—Furosemide (FuroJect, Butler Schein, Dublin, OH) was administered when edema was observed. The dose, frequency, and duration of treatment were at the discretion of the consulting veterinarian. Generally, NHPs were treated with a planned taper as follows: 1.0 mg kg^{-1} QD on the first day of treatment, 0.5 mg kg^{-1} QD for 3 d, and 0.25 mg kg^{-1} QD for 3 d.

Nutritional support—On all days post-irradiation, animals received fresh fruit, soft food, and bottles containing diluted fruit juice or oral rehydration solution (Prang™, Bio-Serv, 1 8th St., Frenchtown, NJ 08825 USA). Animals that lost 10% of their pre-irradiation bw were administered BIO-SERV certified Rhesus Liquidiets (15 mL kg^{-1} by OG). The volume of liquid nutrition was reduced to 7 mL kg^{-1} if the animal was also receiving treated water by OG for hydration.

Blood product support—Whole blood, anti-coagulated with 10% citrate-phosphate-dextrose-adenine (CPD-A) (Sigma-Aldrich, 3050 Spruce St., St. Louis, MO 63103 USA), was obtained from healthy male NHPs that weighed 7.0 kg. Blood was filtered through a 70-μ cell strainer (BD Falcon, BD Biosciences, 21588 Network Place, Chicago, IL 60673 USA) and irradiated to 25.00 Gy (Gammacell® Elite 1000, Best Theratonics, 413 March Rd., Kanata, ON K2K 3G1 Canada) prior to use. Transfusions of whole blood were administered at 7–14 mL kg^{-1}, IV through an 18-μ blood filter (Hemo Nate® Filter, Utah Medical Products, Inc., 7043 South 300West, Midvale,UT84047 USA), when any of the following conditions was observed: platelet count (Plt) < 2,000 μL^{-1}; Plt 20,000 μL^{-1} with hemoglobin count (Hgb) < 6.7 g dL^{-1} or hematocrit (Hct) < 20%; a decrease of 5% in Hct within a 24-h time period that resulted in Hct 25%; a decrease of 7% in Hct within a 24-h time period; or uncontrolled hemorrhage.

Hydration status and fluid support—Hydration status was graded according to a four-tier system. Animals were graded 0 if they had normal hydration. Animals were considered mildly dehydrated, grade 1, if they exhibited any of the following: tacky mucous membranes, capillary refill time (CRT), or skin tent time (STT) 2 but <3 s. Mildly

dehydrated animals were administered a bolus of LRS (10–15 mL kg^{-1} by slow IV push), and RO water (10–15 mL kg^{-1} by OG). Animals were considered moderately dehydrated, grade 2, if they exhibited any of the mild symptoms plus any of the following symptoms: dry mucous membranes, >3% increase in Hct from the previous day (not related to a previous blood transfusion), sunken eyes, or CRT or STT   3 s. Moderately-dehydrated animals were administered a bolus of LRS (20–30 mL kg^{-1}) over 15–20 min by slow IV push, and reverse osmosis (RO) water (7–10 mL kg^{-1} by OG). Animals were considered severely dehydrated, grade 3, if they exhibited any of the mild or moderate symptoms plus any of the following symptoms: pale mucous membranes, >5% increase in Hct from the previous day (not related to a previous blood transfusion), rapid or weak pulse, cold extremities, lethargy, or rapid breathing. Severely-dehydrated animals were administered fluids as described for moderate dehydration, with the addition of an IV infusion of LRS (10–20 mL kg^{-1} h^{-1}) administered over a period of 2–4 h. Animals were placed in a restraint device at this time and allowed to awaken. Midazolam HCl (Bedford Laboratories™, 300 Northfield Rd., Bedford, OH 44146 USA) (0.2 mg kg^{-1} IM or IV) was administered as needed to calm the NHPs while in the restraint.

Euthanasia

Animals were euthanized with DEA Class III euthanasia solution (Euthasol, Virbac AH Inc., 3200 Meacham Blvd., Ft. Worth, TX 76137 USA) (0.27 ml kg^{-1} IV). Expiration was confirmed by a lack of heartbeat, absent femoral artery pulse, and lack of chest respiration. Euthanasia criteria were specified according to IACUC protocol. Animals that exhibited any one of the following conditions were euthanized: inactivity (the animal was recumbent in the cage with decreased or absent responsiveness to touch); weight loss >25% of pre-irradiation body weight for >72 h; hemorrhage from the GI tract or other orifice estimated to be in excess of 20% of estimated blood volume in any 24 h period; severe injury or clinical condition, such as progressive tissue necrosis or severe internal bleeding; SpO$_2$ 88% in the animal's home room air; or hypothermia (rectal body temperature <96°F) for >6 h.

Animals that exhibited any combination of two or more of the following conditions were euthanized: respiratory distress (respiration rate >60 breaths min^{-1} with heart rate <90 beats min^{-1}); weight loss >20% of pre-irradiation body weight for >72 consecutive hours; abnormal activity (e.g., difficulty with ambulation, decreased food and water intake, reluctance to move for >24 h); irreversible clinical condition (e.g., severe dehydration that is non-responsive to IV fluid therapy); shallow respiration; or hyperthermia (rectal temperature >105.5°F) that is unresponsive to antipyretic therapy; abnormal appearance (e.g., rough coat, head down, tucked abdomen, pallor, exudates around eyes or nose).

All surviving animals were euthanized at 180 ± 10 d post-irradiation or at predetermined time points for tissue collection.

Histology

Tissues procured at necropsy were processed for histological analysis. All samples were immersed in 10% neutral-buffered formalin for at least 48 h, embedded in paraffin, cut in 5-μ serial sections, and stained with hematoxylin and eosin (H&E).

GI histology—Jejunum and proximal colon specimens were sectioned into 1–3 cm lengths and flayed open along the anti-mesenteric border. Specimens were pinned flat, mucosal side up, to a silicone base Petri dish containing an elastomer, Sylgard 184 (Dow Corning, 700 2nd St., NE, #8100, Washington, DC 20002 USA).

Crypt survival—The number of surviving and regenerating crypts per length of intestine was scored and the average per group determined. A surviving crypt was defined as one that was tightly packed and contained 10 or more strongly H&E-stained cells (excluding Paneth cells). Only correctly oriented regions that did not contain Peyers patches were scored (Peyers patches influence both the number of crypts in a normal circumference and the ability of a crypt to survive an insult). The size of surviving crypts varied, influencing the likelihood of observing a surviving crypt in cross section, so a size correction factor was applied to reduce this error based on the widths of crypts in non-irradiated control NHPs and surviving crypts in irradiated NHPs (Potten et al. 1981). The corrected number of crypts was calculated according to the following equation:

$$Corrected\ number\ of\ crypts = \frac{mean\ width\ in\ control\ NHP}{mean\ width\ in\ irradiated\ animal} \times (mean\ number\ of\ surviving\ crypts\ in\ the\ irradiated\ animal).$$

Bone marrow histology—Bone marrow cores were extracted from approximately 1.5 cm sections of the tibia and femur.

Lung histology—Lung samples were sectioned into 2–3 cm lengths, extending from the outer edge to inner middle of the lung. Selected lung samples were also stained with Masson's Trichrome.

CT scans and image analysis

The use and standardization of the use of computed tomography (CT) scans to evaluate the latency, incidence, and severity of radiation-induced lung injury in the PBI/BM5 model evolved as the studies were conducted. In theinitial studies, CT scans were performed at 60 ± 5 d post-irradiation, and every 30 ± 5 d thereafter to assess damage. In more recent studies, a pre-irradiation CT scan was performed followed by serial CT scans every 30 ± 5 d post-exposure until the end of each NHP's in vivo phase of the study.

CT scans were acquired using the axial imaging acquisition mode on a Philips Brilliance Big Bore multi-slice CT scanner (Philips Healthcare, 3000 Minuteman Rd., Andover, MA 01810 USA) with a non-contrast enhanced thoracic protocol optimized for lung imaging. The scans were acquired with a slice thickness of 1 mm, a resolution of 0.853 pixels per mm, 120 kilovolt potential. CT images were then digitally archived in Digital Imaging and Communications in Medicine (DICOM) format. Images were analyzed for evidence of radiation-induced lung injury based on characteristic differences in radiodensity of the normal versus damaged lung. The radiographic analysis was performed on a workstation running image analysis software (MIM software suite™ v.5, MIM Software Inc., 25200 Chagrin Blvd. #200, Cleveland, OH 44122 USA). The radiographic incidence and severity of radiation-induced lung injury were calculated for the NHPs on which serial CT scans

were performed. Severity of injury was subjectively scored on a 0–3 scale for each CT scan by an individual with expertise in the field, based on the volume and distribution of pneumonitic and fibrotic lung. A score of 0 was given to any scan with no radiographic evidence of lung injury. Scores of 1, 2, and 3 were given to scans with mild, moderate, and severe evidence of radiation-induced lung injury, respectively.

Experimental endpoints

Primary endpoints—The primary endpoint was all-cause mortality within the timeframes associated with organ-specific and multi-organ morbidity and mortality over the 180-d in vivo phase of the study. The respective acute GI-ARS and combined H-ARS with concomitant GI damage subsyndromes were defined by morbidity and mortality within 15 and 60 d post-exposure. The mean survival time (MST) of decedents was also evaluated.

Secondary endpoints—Secondary endpoints included key parameters associated with GI-, hematological-, lung, and multi-organ-associated injury.

GI- and multi-organ associated parameters included incidence, severity, and duration of diarrhea (stool consistency), dehydration, edema, loss of body weight, gross histological analysis of radiation damage in the jejunum and colon, and crypt counts in the jejunum and proximal colon.

Hematological analysis included neutrophil- and Plt-related parameters, including respective neutrophil and Plt nadirs, the incidence and first day of grade 3 and 4 neutropenia (ANC < 500 μL^{-1} and <100 μL^{-1}, respectively), the incidence and first day of thrombocytopenia (Plt < 20,000 μL^{-1}), and time to recovery to an ANC > 1,000 μL^{-1} and Plt > 20,000 μL^{-1}. Additional parameters included the first day and incidence of febrile neutropenia (FN) and the incidence of documented infection according to blood cultures.

Lung injury was determined by clinical, radiographic, and histopathologic analysis. Clinical parameters included serial, non-sedated respiratory rate and SpO_2 levels. Radiographic analysis was conducted based on serial, non-contrast enhanced, high-resolution CT scans. Gross and microscopic analysis of the lungs were performed. The incidence, latency, and severity of radiation-induced lung injury were calculated and characterized. Survival and MST of decedents in the NHPs experiencing delayed lung injury concomitant with multi-organ injuries were also calculated.

Statistical methods

Mortality—The mortality of rhesus macaques exposed to PBI/BM5 in six dose groups was assessed. Mortality rates were calculated for each dose group and timeframe post-exposure (15 d, $n = 79$; 60 d, $n = 72$; and 180 d, $n = 64$ d), and a dose normal probit fit was made. Confidence intervals on LD quantities and probit slopes were calculated using the methods of Finney (1947). Comparison of slopes and LD50s was made using Wald statistics. All analysis was performed using the R statistical software (version 2.13.1).

The respective mortality data associated with organ-specific and multi-organ subsyndromes identified post PBI/BM5 was compared to contemporary 15-d, 60-d, and 180-d organ-

specific studies focused on GI, hematopoietic, and lung damage that were conducted using TBI or WTLI with the same radiation source, medical management, and statistical analysis (MacVittie et al. 2012; Farese et al. 2012; Garofalo et al. unpublished[§§]).

Descriptive statistics—Continuous data and count data for all secondary parameters were collated and displayed in both tables and graphs. Secondary endpoint parameters were analyzed by both radiation dose and survival outcome where applicable. Animals were grouped into three cohorts according to radiation dose: low (9.0–10.0 Gy),mid (11.0–11.5 Gy), and high (12.0–12.5 Gy). Graphs and tables were constructed using Microsoft® Excel 2007.

RESULTS

The DRR and organ-specific damage consequent to the PBI/BM5 Exposure: Defining the time course for morbidity and mortality for respective organ-specific and multi-organ sequelae of the acute GI-ARS, H-ARS with concomitant GI, prolonged GI-ARS, and the multi-organ DEARE

Acute GI-ARS—The acute GI-ARS is defined as all-cause mortality within 15 d post-PBI/BM5 (MacVittie et al. 2012). The exposure of NHPs to a dose range of 9.0–12.5 Gy resulted in a two-parameter DRR defined by a steep slope of 1.20 [0.58, 1.81] probits linear dose^{-1} and estimated values for the LD30, LD50, and LD70/15 of 11.51 Gy [11.12, 11.85], 11.95 Gy [11.64, 12.51], and 12.39 Gy [12.01, 13.33], respectively (Fig. 2, Table 1). Another measure of the slope is the LD90:LD10. The LD90/15 of 13.02 Gy and LD10/15 of 10.88 Gy yielded a ratio of 1.20 and a dose differential of 2.14 Gy. The MST of decedents across all doses was 9.5 d and the range was 6 to 14 d (Table 2).

Acute GI-ARS: Comparison of PBI/BM5 and TBI DRR—The value for the LD50/15 derived from the DRR for PBI/BM5 protocol is significantly different from that noted for the TBI GI-ARS DRR (MacVittie et al. 2012). The respective LD50/15 value for TBI was 11.33 Gy [10.81, 11.75], relative to 11.95 Gy noted above for PBI/BM5 ($p = 0.023$). The slope for the TBI DRR was 0.92 [0.49, 1.34] probits linear dose^{-1}. This was not significantly different than the slope of 1.20 noted above for the PBI/BM5 DRR ($p = 0.46$). The LD90:LD10 for TBI was 1.28, and the dose differential from 10% to 90% mortality was 2.80 Gy (Fig. 2, Table 1) (MacVittie et al. 2012). The surviving animals from the PBI/BM5 protocol continued to experience unresolved GI damage and the evolving H-ARS.

H-ARS with concomitant GI damage—The morbidity and mortality associated with coincident H-ARS and prolonged GI-damage was defined by survival through 60 d post-PBI/BM5. This DRR was defined by an LD50/60 of 11.01 Gy [10.57, 11.41] and slope of 0.87 [0.48, 1.25] probits linear dose^{-1} (Fig. 2, Table 1). The LD90:LD10 was 1.31, with a dose differential of 2.95 Gy. The MST of all animals ($n = 36$) that succumbed within the 60 d time-frame was 17.6 d and ranged from 6.0 to 53.0 d (Table 2).

[§§]Garofalo, M. NHP WTLI mortality study. Unpublished raw data. Baltimore: University of Maryland; 2012.

H-ARS with concomitant GI damage: Comparison of PBI/BM5 and TBI DR—
The DRR for the H-ARS with concomitant GI damage post-PBI/BM5 is significantly
different from that noted for the H-ARS consequent to TBI (Fig. 2) (Farese et al. 2012). The
LD50/60 of 11.01 Gy for the PBI/BM5 model is significantly greater than the 7.45 Gy
estimated for the composite H-ARS data ($n = 110$) post-TBI ($p < 0.001$) (Fig. 2, Table 1).
The higher LD50/60 value reflects the survival-enhancing effect of sparing 5% of BM.
Recovery of the hematopoietic system was stimulated by regeneration of active
hematopoiesis from the spared tibiae-derived BM, which received an average dose of 0.53
Gy. The consequent degrees of neutropenia and thrombocytopenia were diminished along
with the risk of sepsis and inopportune hemorrhage. Recovery of the hematopoietic system
was measured by regeneration of peripheral blood neutrophils and platelets to normal levels.
The long-term recovery of the hematopoietic system relative to replenishment of functional
hematopoietic stem cells (HSC) and progenitor cells (HPC) was not determined.
Histological examination of marrow confirmed the rationale of sparing the tibiae and
exposing the remaining marrow to high-dose irradiation (Fig. 3). On day 17 post-PBI/BM5,
the marrow procured from the tibiae was replete with hematopoietic cells as compared to
hypo-cellular femoral marrow. Recovery of marrow hematopoiesis is evident in the femur,
but the marrow space is not replete with active sites as seen in the normal femur or tibia.

The DRR of the TBI-induced H-ARS indicated that 8.9 Gy, plus supportive care is 100%
lethal (Farese et al. 2012). However, the PBI/BM5 DRR indicated that lethality would be
<5% at 9.0 Gy with the same standard of care. An estimated dose modification factor (DMF)
for the BM-sparing effect for respective LD50 values for TBI H-ARS and the PBI/BM5 H-
ARS with concomitant GI damage is approximately 1.48, while the DMF is equivalent
(1.05) for the acute GI-ARS LD50/15 values derived from the TBI (11.33 Gy) and PBI/BM5
(11.95 Gy) models.

In summary, the PBI/BM5 protocol had a significant effect on modulating the associated
mortality consequent to the acute GI-ARS, resulting in a higher value for the LD50/15.
However, the respective slopes were not significantly different. The cohorts surviving the
acute GI-ARS continued to experience prolonged GI damage and multi-organ injury. Overt
lung injury was imminent in the low- to mid-dose cohorts, whereas GI and injury to other
organs predominated in the high-dose cohort, increasing morbidity and mortality; i.e., earlier
mortality from multi-organ injury prevented the expression of lung injury (Table 2).

**Multi-organ injury characteristic of the DEARE: Co-morbidities and mortality
—**Morbidity and mortality associated with bw loss, edema, lung injury, and continued GI
damage is defined over the total 180-d time course post-PBI/BM5. The DRR for the
survivors of the acute GI-ARS (day 15) and H-ARS with concomitant GI damage (day 60)
through 180 d was defined by an LD50/180 of 9.73 Gy [8.91, 10.17] (Fig. 2, Table 1) and a
slope of 1.14 [0.58, 1.71] probits linear dose^{-1}. The LD90:LD10 was 1.26 with an LD10 to
LD90 dose differential of 2.24 Gy. The MST of decedents across all doses was 50.8 d (Table
2).

In summary, the slopes of respective DRRs for the acute GI-ARS (1.20), H-ARS with
concomitant GI damage (0.87), and multi-organ injury (1.14) post-PBI/BM5 were

comparably steep (Table 1, Fig. 2). The range of the dose differential between 10% and 90% mortality was 2.24 to 2.95 Gy, and the LD10:LD90 ranged from 1.26 to 1.31.

GI-ARS-related secondary parameter: the acute and prolonged time course

Dehydration—Three dose cohorts were selected for data analysis: low (9.0–10.0 Gy), mid (11.0–11.5 Gy), and high (12.0–12.5 Gy). All NHPs across all dose ranges experienced dehydration to a moderate degree (grade 2) within 10 d post-PBI/BM5 (Fig. 4, Table 3b), reaching that level by day 6 on average. The mean level of dehydration was mild to moderate through 30 d, improving thereafter to normal hydration within 80 to 100 d post-exposure. A dose-dependent increase in the degree of dehydration was noted. The percentage of animals that became severely dehydrated increased across the low, mid, and high dose cohorts, with incidence of 25%, 41%, and 76%, respectively (Table 3a).

Edema—Edema in the scrotum and lower abdomen was observed in 23% of all animals. The mean first day such edema was observed was day 78 post-exposure, ranging from day 34 to 111. The edema was prolonged and persistent, lasting up to 93 d among animals that survived to recovery.

Body weight loss and recovery—All NHPs experienced decreased bw post-exposure, reaching 10% loss of pre-irradiation bw by day 9 on average (Table 4b). There-after, bw continued to decrease in all three dose cohorts, with each cohort reaching their respective mean nadirs within 20 to 30 d (Fig. 5). The low-dose cohort experienced full recovery to pre-exposure bw within 60 d post-exposure. The high-dose cohort remained at approximately 20% below pre-irradiation bw through day 60 and continued to lose weight until euthanasia was required. There is a clear distinction in bw loss between survivors and decedents throughout the time course of the study (Fig. 5b). Following a recovery phase, decedents experienced a subsequent severe loss through the end of their in vivo phase, while on average survivors maintained their bw after the recovery phase.

Incidence of diarrhea and stool consistency—All NHPs developed diarrhea post-PBI/BM5 in a timeframe similar to that noted post-TBI (MacVittie et al. 2012). The mean first day of diarrhea (grade 2 stool consistency) across all dose cohorts was 4.3 d post-exposure (Table 5b), with mean stool consistency values peaking at day 7. Sixty-five percent of animals experienced bloody stool during the acute GI-ARS time course, with incidence decreasing thereafter (Fig. 6). Mean stool consistency grades began to decrease in the second week post-exposure with an apparent dose-dependent delay. Animals in each dose cohort experienced intermittent episodes of diarrhea throughout the in vivo phase of the study.

GI histology

Animals exposed to 10.0 Gy PBI/BM5 were euthanized at predetermined time points across the 180 d in vivo phase to evaluate the degree of recovery of numbers of crypts and crypt and villus architecture in animals that had not met euthanasia criteria. The 10.0 Gy dose was selected for histological analysis of GI damage because it is an approximate threshold dose for the acute GI-ARS. Additionally, few animals would succumb during the in vivo phase,

allowing a more complete analysis of all tissues and secondary parameters of coincident sequelae over 180 d.

Histological analysis was performed on the jejunum and proximal colon from non-irradiated NHPs ($n = 11$) and irradiated NHPs at the following days post-exposure: 7, 34, 44, 61, 99, and 180.

Damage and recovery of crypts in the jejunum—Early crypt loss at day 7 allowed comparison with the crypt loss noted in the TBI model (MacVittie et al. 2012). The mean number of crypts mm^{-1} at day 7 post-PBI/BM5 and TBI were 4.0 and 3.7, respectively, which was approximately 28% of the non-irradiated mean value of 13.7. Thereafter, the mean crypt count increased to approximately 44% of the non-irradiated value between days 34 to 61, to 66% at day 99, and 70% at day 180 (Fig. 7a). Recovery of crypts in the jejunum was prolonged, remaining below non-irradiated values throughout the 180 d time course. A smaller data set was collected for analysis of crypt damage and recovery consequent to 11.5 Gy PBI/BM5 using animals euthanized for meeting euthanasia criteria. These data suggested severe depletion of crypts to approximately 9% of non-irradiated levels at day 8, with a single animal analyzed at day 169 recovering to 63% (data not shown).

Damage and recovery of crypts in the proximal colon—The average number of crypts mm^{-1} for the non-irradiated proximal colon was 11.92. Within 7 d post-exposure, this value was decreased to 4.44, 37% of the non-irradiated value (Fig. 7b). Thereafter, the mean crypt count increased to approximately 65% of the non-irradiated value between days 34 to 61, to 90% at day 99, and then decreased to 81% at day 180. This suggests a similar time course of recovery as observed in the jejunum, though more pronounced recovery appeared to occur earlier in the proximal colon. The data collected for the 11.5 Gy cohort also reflected a similar time course to that noted for the 10.0 Gy cohort. Crypts were severely depleted to approximately 12% of non-irradiated values at day 8, while counts in two animals euthanized at days 114 and 169 were both greater than the non-irradiated means (data not shown).

GI histopathology: crypt and villus architecture—There were progressive changes in the appearance of the jejunum and proximal colon post-exposure. In the jejunum, the following observations were made in comparison to non-irradiated tissue: by day 7 there was loss of villi, reduced numbers of crypts, submucosal edema, and thickening of the *muscularis mucosa*; by day 34, crypt depth and regeneration was increased, but in the absence of villus reconstitution; by days 61 and 99, villi were present with an increased number of mucus-secreting goblet cells and crypt regeneration continued, marked by hyperplasia and bifurcation (Fig. 8a). The proximal colon presented a similar course and pattern of damage, with loss of surface epithelial cells and crypts, early submucosal edema, crypt hyperplasia by day 61, and increased numbers of goblet cells that persisted through day 180 (Fig. 8b). Hemorrhage was noted in both the jejunum and proximal colon in animals throughout the time course. Cellularity in the *lamina propria* was decreased on day 7 compared to non-irradiated tissue, but increased numbers of cells surrounding the crypts from day 34 onwards suggest persistent inflammation.

The characteristic features in the intestinal tissues suggest a prolonged lack of mucosal restitution, a prolonged time course of crypt regeneration and reconstitution, and a marked increase in goblet cells. The dysregulated and prolonged period of recovery may result in poor nutrient uptake, diminished fluid reabsorption, and secretory diarrhea, consistent with the clinical observations detailed above.

H-ARS with concomitant GI damage-related secondary hematological parameters

The time course, incidence, and severity of neutropenia and thrombocytopenia—PBI/BM5 exposures across all dose cohorts induced grade 3 neutropenia (ANC < 500 μL^{-1}) and thrombocytopenia (Plt < 20,000 μL^{-1}). The ANC and Plt nadirs occurred on days 6 and 11, respectively. The ANC fully recovered to normal, pre-irradiation values within approximately 30 d, while the full Plt recovery to normal values occurred within approximately of 60 d post-exposure (Fig. 9).

Neutrophil-related parameters: PBI/BM5 versus TBI—PBI/BM5 exposure induced grade 3 neutropenia in all but one animal. The mean first day of neutropenia was 4.6, and the mean first day of recovery ranged from 18.6 to 25.6 (Table 6). In comparison, TBI at 7.2 to 8.9 Gy induced neutropenia of longer duration, with the mean first day of recovery ranging from 21.7 to 42.0 d (Farese et al. 2012).

Sixty-one percent (61%) of all NHPs exposed to PBI/BM5 protocol experienced grade 4 neutropenia (ANC <100 μL^{-1}) by day 6.2 on average, approximately 2 d after reaching grade 3 (Table 6). The mean duration of grade 4 neutropenia was 4.9 d. In comparison, TBI at 7.2 to 8.9 Gy produced a longer duration of grade 4 neutropenia that ranged from 9.8 to 12.7 d (Farese et al. herein). The comparative radiation-induced neutropenia for PBI/BM5 versus TBI of approximately equivalent (9.0 versus 8.9 Gy) or lesser (7.5 Gy) dose is used to illustrate the pronounced effect on hematopoiesis and recovery of neutrophils consequent to 5% BM sparing (Fig. 10a). The 8.9 Gy and 7.5 Gy doses of TBI are 100% and 50% lethal, respectively. The 9.0 Gy dose of PBI/BM5 is sublethal for H-ARS with concomitant GI damage.

Febrile neutropenia (FN) and fever—The mean first day of FN was 13.6 and 15.9 in the low- and mid-dose cohorts, respectively (Table 7). The high-dose cohort could not be evaluated due to early lethality; only 1 of 21 high-dose animals had FN, whereas 56% and 33% of the low-and mid-dose animals had FN, respectively. Respective positive blood cultures were noted in 25% and 19% of the low- and mid-dose cohorts. Fever was not observed in animals following recovery of neutrophils to >500 μL^{-1} through the in vivo phase (data not shown). In comparison, 91% of all animals exposed to TBI doses in the H-ARS range of 7.2 to 8.9 Gy experienced FN relative to the 56% and 33% noted above for the PBI/BM5 protocol. Additionally, the mean first day to FN for all cohorts was 8.7 relative to 13.6 d and 15.9 d noted above for the PBI/BM5 protocol (Farese et al. 2012).

Platelet-related parameters: PBI/BM5 versus TBI—Animals across all three dose cohorts became moderately thrombocytopenic. Mean Plt nadirs between 10,000 to 20,000 μL^{-1} occurred on approximately day 11 post-exposure (Fig. 9, Table 8). The mean duration

of thrombocytopenia across all dose cohorts was 9.4 d. At least one whole blood transfusion was required in 28% of the animals, with a mean first day of transfusion of 11.6.

In comparison, 98% of all animals exposed to TBI doses in the H-ARS range of 7.2 to 8.9 Gy required at least one transfusion. Similar to the PBI/BM5 animals, the mean first day of transfusion was 12.1 post-TBI (Farese et al. 2012). The comparative radiation-induced thrombocytopenia for PBI/BM5 versus TBI of approximately equivalent (9.0 versus 8.9 Gy) or lesser (7.5 Gy) dose illustrates the marked effect on thrombopoiesis and recovery between the two exposure geometries (Fig. 10b).

Lung injury within coincident multi-organ associated parameters

Radiation pneumonitis: incidence and latency—The latency to development of clinical pneumonitis was calculated based on the elapsed time from initial radiation exposure to development of tachypnea and respiratory distress [defined as a non-sedated respiratory rate (NSRR) of >80 bpm in room air]. Therefore, this analysis was restricted to NHPs for which complete, serial NSRR data were available among those NHPs who survived the latent period for lung injury, during which mortality from acute GI-ARS and H-ARS coincident with prolonged GI damage occurs (i.e., animals surviving >60 d). Of the 64 NHPs exposed to PBI/BM5 doses between 9.0 and 12.5 Gy and observed for up to 180 d, there were a total of 28 NHPs who survived >60 d, of which 15 had NSRR data sufficient for analysis. The incidence of pneumonitis and mean latency to development of pneumonitis was calculated for each radiation dose cohort. The mean latency reported was calculated from only the NHPs that developed pneumonitis. All animals defined clinically as having developed pneumonitis had correlative radiographic injury evident by computed tomography. At doses above 11.5 Gy, there were two NHPs that survived >60 d, but neither had NSRR data sufficient for analysis. Clinical pneumonitis was observed at all PBI/BM5 doses available for analysis (9.0–11.5 Gy). Its incidence increased with dose of exposure (9.0 up to 11.0 Gy); however, the incidence of pneumonitis was lower in the 11.5 Gy cohort, which may be a result of two of the three animals in this cohort being euthanized on days 76 and 77 post-exposure, thus not surviving long enough to develop pneumonitis. The mean latency to development of clinical pneumonitis was not significantly different between the different exposure dose groups (99.8 d for 11.0–11.5 Gy versus 99.7 d for 9.0–10.0 Gy) (Table 9).

Evaluating lethality for survivors of the GI-ARS and H-ARS coincident with prolonged GI damage (NHPs at risk for mortality from lung-DEARE and/or prolonged GI damage)—For the 28 NHPs that survived the GI-ARS and H-ARS (e.g., >60 d), the survival rate and the MST of decedents were calculated. The data suggested that as exposure dose increased, the survival rate and MST of decedents decreased. Survival rates past 60 d were 67%, 14%, and 0% in the low-, mid-, and high-dose cohorts, respectively (Table 9). The mean survival time of decedents in the low-, mid-, and high-dose cohorts were 143.5, 123.8, and 91.5 d post-exposure, respectively. The threshold dose at which lethality due to pneumonitis began to be seen was 10.0 Gy in the PBI/BM5 model. There were no survivors (0/7) at PBI/BM5 exposure doses of 11.5 Gy and above.

Nonsedated respiratory rate and dexamethasone treatment—NSRR were recorded daily for a portion (n = 15/28) of the NHPs who survived the GI-ARS and HARS coincident with prolonged GI. The mean NSRR for each exposure dose cohort was calculated and graphed over time (Fig. 11). The mean NSRR for the high-dose cohorts (n = 2) could not be calculated, as these data were not available. The mean NSRR was not significantly different between the low- and mid-dose exposure cohorts, but for both cohorts it demonstrated that radiation-induced lung damage is clinically silent for approximately 2 mo following partial-body irradiation. The mean NSRR increased steadily beginning at 2 mo post-exposure, reaching a peak at approximately 115 d post-exposure. Downward trends in mean NSRR beyond day 115 post-exposure are explained by 1) effective treatment with supportive care (corticosteroids) and 2) continued lethality of the most severely affected NHPs. Of the NHPs surviving at least 60 d, dexamethasone support was provided to 42% (5/12) of the NHPs in the low-dose cohort, beginning on 113.2 d post-exposure on average. By contrast, 50% of the NHPs in the mid-dose cohort received dexamethasone beginning on day 115.1 on average. The two NHPs in the high-dose cohort did not receive dexamethasone. The timing of dexamethasone treatment correlates with changes seen in NSRR and subsequent CT scans.

Radiographic assessment of radiation-induced lung injury—Serial non-contrast enhanced CT scans were obtained to assess the time-course, incidence, and severity of radiation-induced lung injury radiographically. As the PBI/BM5 model evolved, the timing and frequency of CT scans was standardized to be every 30 d post-exposure. The severity of radiographic injury was subjectively scored based on the volume and distribution of pneumonitic and fibrotic lung parenchyma as represented by characteristic changes in radiodensity. The CT scans were qualitatively scored as being normal (score 0), with mild damage (score 1), with moderate damage (score 2), or with severe damage (score 3) by a thoracic radiography expert (Fig. 12).

This analysis was restricted to NHPs for whom serial CT data were available among those NHPs who survived the GI-ARS and H-ARS with coincident GI damage (e.g., >60 d post-exposure). Of the 64 NHPs who were exposed to PBI/BM5 and followed for up to 180 d, there were a total of 28 NHPs who survived >60 d, of which 24 had CT data sufficient for analysis. The incidence of radiographic lung injury was calculated for each dose cohort at every time point at which CT scans were taken. The incidence of radiographic injury increased both as a function of time and exposure dose (Table 10). At doses of 11.0 Gy and above, all NHPs manifested radiographic evidence of lung injury during the study. The mean severity score of radiographic injury (considering only the CT scans with evidence of injury) was calculated for each dose cohort and at each time point at which CT scans were taken (Fig. 13). For NHPs with radiographic evidence of injury, the mean severity score reached an initial peak at day 90 in the low-and mid-dose cohorts, which correlates with the clinical NSRR data. Reductions in mean severity scores at day 120 post-exposure are likely explained by the influence of 1) corticosteroid treatment (causing consequent reductions in NSRR and decreased volume of radiographic injury on CT) and 2) continuing lethality of NHPs with the greatest lung injury despite supportive care. On average, dexamethasone was administered initially between day 113–115 post-exposure. Therefore, the results of the

scans taken at days 30, 60, and 90 are largely free of the confounding variable of dexamethasone (Fig. 14).

Lung histopathology—Typical findings in the irradiated NHPs included macrophage infiltration with foamy macrophages, thickening of the alveolar walls and inter-alveolar septae, distortion of alveolar architecture, hyaline membrane formation in alveolar airspaces, and collagen deposition indicative of evolving fibrosis (Fig. 15).

DISCUSSION

The reality of the nuclear accident or terrorist scenario

Radiation accident scenarios have provided several defining characteristics useful in the design of emergency preparedness models and treatment strategies for severely irradiated personnel who develop the ARS as well as the DEARE (MacVittie et al. 1996; Ricks and Fry 1990; Baranov et al. 1994; Liu et al. 2008; Gourmelon et al. 2010; Hirama et al. 2003; Igaki et al. 2008). The radiation environment after a nuclear terrorist event will be ill-defined as a result of body position relative to the source, random shielding, distance from the source, and variable dose rate in the fallout field. These factors predict a non-uniform, unilateral, and heterogeneous exposure. The only optimistic aspect for those exposed to potentially lethal doses of radiation is that the above characteristics forecast a highly variable dose distribution to the body with consequent sparing of stem and progenitor cells in the hematopoietic and GI systems. The tissue-sparing aspect of radiation exposure will enhance the potential for survival and amelioration of life-threatening subsyndromes (Monroy et al. 1988; Bond and Robinson 1967; Cole et al. 1967; Hansen et al. 1961; Maillie et al. 1966; Wang et al. 1991; Baltschukat and Nothdurft 1990; Bertho et al. 2005a; Bertho et al. 2005b; Bond et al. 1991; Rauchwerger 1972). Supportive care alone will enhance MST in this scenario and provide time for spontaneous and treatment-induced, tissue-specific regeneration of respective organ systems (Jackson et al. 1959; MacVittie et al. 1991; Perman et al. 1962; Bagdasarov et al. 1959; Thomas et al. 1962; MacVittie et al. 2005; Conard et al. 1956; Taketa 1962).

An animal model research platform

Understanding the radiation exposure scenario is essential to defining the requirements for relevant animal models that mimic the human response to acute, high dose, potentially lethal radiation exposure and its treatment (MacVittie et al. 1996; Ricks and Fry 1990; Baranov et al. 1994; Liu et al. 2008; Fliedner et al. 2007; Konchalovsky 2010; Hirama et al. 2003; Igaki et al. 2008). The rationale for establishing the animal model research platform is based on several requirements. These are: a) to evaluate and understand the key organ-specific and multi-organ sequelae that are survivable in a realistic nuclear radiation scenario (e.g., the GI-ARS, H-ARS, prolonged GI damage and delayed multi-organ injury and lung injury); b) to define the radiation dose-, incidence, severity and time-dependent relationships for each subsyndrome and sequelae; c) to determine how to model the key sequelae in a linked fashion (the ARS and DEARE are composites of dose- and organ-specific damage that may occur in coincident and/or sequential manner); and d) to develop a model that will permit definition of concomitant organ-specific damage that is essential to rational development of

a MCM poly-pharmacy approach to treat potentially lethally irradiated personnel. Organ-specific MCM may have significant effects on the incidence and severity of damage to other organs, complicating assessment of the efficacy of combination MCM for two or more sequelae. The PBI/BM5 model will provide invaluable insight into the interaction and potential causal relationships between the linked and coincident sequelae of the ARS and DEARE.

Sparing hematopoietic or GI tissue: Effect on organ-specific regeneration and survival

The aim of sparing 5% BM was to maintain the mortality and morbidity associated with the acute GI-ARS induced by TBI while preserving enough active BM to ensure dose-dependent survival through the evolving H-ARS and coincident prolonged GI damage. Sparing BM or GI tissue through shielding, partial-body exposure, or unilateral exposure effectively preserves the regenerative integrity of hematopoietic stem and progenitor cells (HSC, HPC) or intestinal crypts or amplifying progenitor cells (Monroy et al. 1988; Bond and Robinson 1967; Cole et al. 1967; Hansen et al. 1961; Maillie et al. 1966; Wang et al. 1991; Handford et al. 1961; Bertho et al. 2005a; Bertho et al. 2005b; Bond et al. 1991; Rauchwerger 1972; Taketa et al. 1959).

Hematopoietic tissue sparing

Several studies suggested that a) sparing a relatively larger percentage of BM (or BM transplant) enhanced resistance of animals to the lethal GI-ARS (Vriesendorp et al. 1992; Terry and Travis 1989; Mason et al. 1989; Handford et al. 1961), b) anecdotal data from nuclear accidents dictated that the exposures were non-uniform and heterogeneous with some degree of BM and GI tissue sparing (MacVittie et al. 1996; Ricks and Fry 1990; Baranov et al. 1994; Liu et al. 2008; Konchalovsky et al. 2005; Gourmelon et al. 2010; Hirama et al. 2003; Igaki et al. 2008); and c) the mortality due to the acute H-ARS is due to the radiation dose to the BM and survival of stem and progenitor cells. Bond and Robinson originally suggested that survival from the acute H-ARS is dependent on the dose-dependent survival of a critical fraction of the BM stem cells (Bond and Robinson 1967). This hypothesis assumed that: a) the dose-effect curve for sterilization of HSC and HPC is closely approximated by an exponential function over the range of the acute H-ARS DRR; b) BM-derived HSC and HPC were distributed in equivalent fashion throughout the active BM sites of the body; c) a surviving HSC/HPC will contribute to regeneration of the hematopoietic system at a rate that is independent of their anatomic location; and d) each species has its own critical fraction of HSC and HPC in the BM. Species differences such as HSC quiescence, concentration of HSC/HPC, total BM cellularity, and turnover may affect the DRR and recovery parameters (Bradford et al. 1997; Traycoff et al. 1998; Broerse and MacVittie 1984; Cheshier et al. 1999; Mahmud et al. 2001; van Bekkum 1991). The Bond and Robinson model predicted that for the acute H-ARS, survival depends on the same critical surviving fraction of HSC/HPC following uniform or non-uniform exposure (Bond and Robinson 1967; Bond et al. 1991).

The effect of several variables on survival and the DRR must be acknowledged: a) supportive care enhances survival by providing longer survival time post-exposure via replacement/substitution therapy with antibiotics, fluids, and transfusions (the increased

survival time extends that required for production of neutrophils and platelets within that critical clinically manageable period of time post exposure); and b) the potential role of the osteoblastic or vascular niche in modifying survival and regeneration of hematopoiesis (Scadden 2006; Calvi et al. 2003; Morrison and Spradling 2008). The role of the BM niche is assumed to be similar to that for HSC/HPC throughout the BM tissue. Therefore, in this model it is possible that the dose range of 9.0 to 12.5 Gy, being myeloablative, may have marked effects on the long-term reconstitution of the hematopoietic system. Long-term "reconstitution" as opposed to "recovery" of the system's ability to support normal homeostasis (i.e., normal levels of neutrophils and platelets) may be compromised due to mobilization, forced cell cycling, altered homing, engraftment, and regulation of the tibiae-derived HSC/HPC within the irradiated vascular and osteoblastic niches (Jang and Sharkis 2007; Dominici et al. 2009; Wang et al. 2010; Carbonneau et al. 2012). The potential long-term residual injury to the HSC population(s) and/or the marrow niches may compromise the ability of the hematopoietic system to respond to subsequent challenges (Orschell et al. 2012).

PBI/BM5 exposure: the DRR for the acute GI-ARS, H-ARS plus coincident GI damage, Multi-organ DEARE and lung injury

The DRR for acute GI-ARS—The DRR for the acute GI-ARS consequent to TBI was defined by an LD50/15 of 11.33 Gy and a slope of 0.92 probits linear dose^{-1} (MacVittie et al. 2012). The DRR for the acute GI-ARS noted in the PBI/BM5 model was 11.95 Gy with a slope of 1.20 probits linear dose^{-1}. The LD50/15 values were significantly different from each other ($p = 0.022$), while the slopes were not, $p = 0.46$. The data suggested that the PBI/BM5 model as established does alter the DRR of the acute GI-ARS. However, the analysis of crypt damage and recovery suggested an equivalent degree and time course of injury. It is of interest that sparing only 5% of active BM would influence the lethal time course of the acute GI-ARS. The results are of value in that they suggest the use of MCM against the H-ARS may also positively affect recovery from the GI-ARS. These effects are also suggested in the initial database provide by the Booth et al. in the mouse model of PBI/BM5 (Booth et al. 2012).

The DRR for H-ARS with coincident GI damage: 60-d mortality—As expected, the relative DRR for the PBI/BM5-induced H-ARS with coincident GI damage was significantly different from that noted for the H-ARS induced by potentially lethal doses of TBI (Farese et al. 2012). At 50% mortality over 60 d, the LD50/60 for TBI was 7.45 Gy, whereas that estimated herein for PBI/BM5 exposure was 11.01 Gy. However, the respective slopes for the DRRs were not significantly different, at 1.05 and 0.87 probits linear dose^{-1} ($p = 0.65$). The survivors through day 60 post-PBI/BM5 have survived the dose-dependent acute GI-ARS and entered the evolving H-ARS in concert with concomitant prolonged GI damage. It must be expected that the prolonged GI damage has contributed to the morbidity and mortality of the H-ARS in this model. However, the reduced severity and accelerated recovery of the hematologic parameters markedly reduced the consequences of the neutropenia and thrombocytopenia. Only 42% of the combined low- and mid-dose cohorts (9.0–11.5 Gy) that enter the H-ARS experience FN due to recovery of neutrophils. Fever in the absence of neutropenia was minimal. In comparison, 91% of the total animals

exposed to TBI in the range of 7.2 to 8.9 Gy experienced FN (Farese et al. 2012), while the GI damage in those animals, albeit evident, was less severe than that noted post-PBI/BM5 exposure. This suggests a relative key role for the neutrophil in maintaining host defense against opportunistic bacteria between these two models. Neutrophil number and function in this case trumps assumed loss of mucosal barrier integrity. Barrier integrity and function remains to be defined along the time course of prolonged GI damage. Histological samples revealed all grades of damage from mild to severe in the small and large intestine through day 180 post-PBI/BM5.

Platelet recovery also reflected the enhanced hematopoietic response from the spared 5% of BM. Only 30.2% of all animals exposed in the low- and mid-dose cohorts (9.0 to 11.5 Gy) of the PBI/BM5 protocol required at least one transfusionversus 98% of all animals in the TBI cohorts.

Bertho and colleagues used a similar PBI protocol to investigate the effect of autologous cell therapy or G-CSF administered within 6 h post-exposure on hematopoietic recovery in nonhuman primates (Bertho et al. 2005a and b). They used doses of 8.0, 8.7, and 10.0 Gy with a partially shielded right arm that was exposed to 3.4 to 4.4 Gy. Hematopoietic recovery was observed in all 8.0 and 8.7 Gy animals, while partial recovery was observed in the 10.0 Gy cohort. They did not intend to develop a DRR for either H-ARS or GI-ARS, but it is noteworthy that consequent to the 10.0 Gy exposure, two of four animals succumbed to GI damage. NHP model development for PBI/BM5 was initially focused on assessing recovery from the acute GI-ARS. All animals (with the exception of a single, unexplained early lethality) survived after 9.0 Gy PBI/BM5. There was approximately 5% mortality due to the acute GI-ARS within the 15-d timeframe at 10.0 Gy PBI/BM5, whereas approximately 15% succumbed within the 60-d timeframe for the combined H-ARS with coincident GIdamage. Exposure to TBI at 8.9 Gy was 100%lethal within the H-ARS (Farese et al. 2012).

Acute radiation damage and prolonged recovery of GI tissue: Intestinal stem cells—Does the GI system recover from potentially lethal doses of radiation within the acute DRR? The answer required a model that permitted recovery of the hematopoietic system following exposure to doses of radiation that are myeloablative and 100% lethal in the TBI model.

The intestinal epithelium is a most rapidly self-renewing tissue, requiring incessant production of enterocytes as well as goblet, Paneth, and enteroendocrine cells. Self-renewal and proliferation of intestinal stem cells (ISC) occurs in the crypts with an epithelial transit time from crypt to the villus tip of approximately 3 d in the mouse and 7 d in the NHP (MacVittie et al. 2012). The identity of the ISC within the crypt has lacked resolution due to inadequate accessibility and a lack of specific markers and appropriate mouse models. Potten provided experimental support for ISC residing in the +4 cell position in the crypt (Potten 1974, 1977). This location was challenged by subsequent studies suggesting that the ISC were located at the base of the crypt between the Paneth cells and crypt base columnar cells (CBC) (Cheng and Leblond 1974; Bjerknes and Cheng 1999). Most recently, two principal ISC have been identified. One population was identified as Lgr5+ cells in the small

intestine and colon, whereas the marker Bmi1 was found present on putative ISC in the small intestine and residing at the +4 position above the Paneth cells (Barker et al 2007; Sangiorgi and Capecchi 2008; Tian et al. 2011). It is believed that these ISC are multipotent and have a functionally distinct relationship in maintaining normal homeostasis and response to injury (Yan et al. 2012; Tian et al. 2011; Kim et al. 2012). The Lgr5+ columnar cells are actively cycling and reside at the crypt base, whereas the Bmi1+ cells are slowly cycling or quiescent and only observed in the small intestine.

Recent experiments by Tian et al. and Yan et al. identified these two ISCs as functionally distinct populations (Yan et al. 2012; Tian et al. 2011). Tian et al. used a diphtheria toxin gene knocked into the Lgr5 locus. They found that complete loss of Lgr5-expressing cells did not perturb homeostasis of the epithelium, suggesting that the Bmi1 population compensated for the loss of Lgr5+ cells. The Bmi1-expressing cells gave rise to Lgr5+ cells, suggesting a hierarchical relationship. Yan et al. used a high-dose radiation model exposing mice to 12 Gy to further investigate differences between these ISC (Yan et al. 2012). They found that the Lgr5+ cells were relatively radiosensitive and ablated at 12 Gy exposure. The Bmi1+ cells were radioresistant and rapidly proliferated with significant contribution to the epithelial regeneration and expansion of downstream progeny into crypts and villi. These data suggest that the Bmi1 subset may represent a reserve ISC pool and source of replenishment for Lgr5+ cells. It can only be speculated that the ISC populations in the NHP retain the same functional properties noted in the murine models. In this case, the damage and prolonged recovery process may reflect dysfunctional repair and renewal of Bmi1 cells, limiting their ability to replenish the Lgr5+ and +4 position cells. The prolonged damage may also reflect a persistent, chronic inflammatory state within the GI tissue as well as a dysfunctional niche leading to aberrant signals for crypt self-renewal and appropriate crypt and villus architectural relationships.

The DRR for multi-organ DEARE with coincident acute GI-ARS, H-ARS with coincident GI damage, and lung injury—The lung is a relatively radiosensitive organ, similar in its threshold dose to the GI system (Van Dyk et al. 1981; Hill 2005). The LD50/180 in animal models varies with species and strain but generally falls between 10.0 Gy and 14.0 Gy for single acute doses of ionizing radiation (Liao et al. 1995; Down and Steel 1983; Franko 2010; Newcomb et al. 1993). Although the threshold for pneumonitis in man is approximately 8.0 Gy, the lethal dose is approximately 10.0 Gy (Marks et al. 2003; Van Dyk et al. 1981). There are no published, well-characterized models in the canine or NHP that define the time course and DRR of the major morbidity and mortality for delayed lung injury following either PBI/BM5 or WTLI. Lethality due to DEARE in the PBI/BM5 model is acknowledged to be a function of both the prolonged GI syndrome and the delayed lung injury. To study and isolate the lung-DEARE from the GI-ARS, H-ARS, and prolonged GI syndromes, a WTLI model was recently developed and characterized in the NHP (Garofalo et al. [§§]). Comparison of outcomes in these two models provides insight into how the earlier H-ARS and GI syndromes may modulate the time course and severity of delayed lung injury. The LD50/180 for lung-DEARE consequent to WTLI is 10.28 Gy. The slopes of the dose-response curve for 180-d mortality in both the PBI/BM5 and the WTLI models are equivalently steep (1.14 probits linear dose^{-1} for both), and the differences in the

LD50/180 between the two models is only 0.55 Gy. This suggests that the NHPs that succumb to radiation-induced H-ARS and GI sequelae in the PBI/BM5 model may have been largely destined to succumb to lung injury had they survived these earlier syndromes. As in the WTLI model, no NHPs were euthanized due to delayed lung injury following an exposure of 9.0 Gy in the PBI/BM5 model. With the acknowledgement that there were no NHPs exposed to 9.5 Gy in the PBI/BM5 model, the threshold dose at which lethal lung injury began to manifest was 9.5 Gy in the WTLI model and 10.0 Gy in the PBI/BM5 model. This suggests that the additional morbidity and mortality contributed by the hematologic and GI syndromes during the latent phase of delayed lung injury did not appreciably alter the threshold dose at which potentially lethal delayed lung injury manifests following PBI/BM5 exposure.

In the PBI/BM5 model, no NHP developed clinical pneumonitis nor was a NHP euthanized for hypoxia or respiratory distress criteria prior to 60 d post-exposure. The mean latency to development of clinical pneumonitis was approximately 100 d post-exposure in the PBI/BM5 model and was not significantly different as a function of dose. This stands in contrast with the WTLI primate model where latency to development of pneumonitis was inversely proportional to dose, ranging from 119.4 d (9.5 Gy WTLI exposure) to 62.8 d (12.0 Gy WTLI exposure), and with the human clinical experience where latency to pneumonitis following fractionated radiation to the lung has been reported to be dose dependent (Ikezoie et al. 1988). This difference may be partially explained by the relatively low number of NHPs in the PBI/BM5 model who survive the competing GI-ARS and H-ARS in the higher dose cohorts and go on to survive the prolonged GI syndrome long enough to manifest lung-DEARE. For example, at the highest dose of PBI/BM5 exposure for which serial NSRR data was collected (11.5 Gy), two of the three NHPs that survived beyond 60 d expired before day 80 post-exposure secondary to the prolonged GI syndrome. The other factor limiting the sample size to evaluate lung-DEARE in the PBI/BM5 model was the evolving nature and focus of the model. The PBI/BM5 model was developed to study the prolonged GI syndrome but evolved into a comprehensive model to study the acute GI-ARS, H-ARS, prolonged GI injury, and lung injury. As a result, early PBI/BM5 studies did not routinely measure all respiratory endpoints (e.g., NSRR, SpO2, CT scans). Despite these limitations, the mean latency to development of clinical pneumonitis in the PBI/BM5 model compares favorably with that reported in humans. In a unique human experience, 245 metastatic cancer patients received single high-dose, midplane exposures of upper half body (UHBI) ^{60}Co gamma radiation of between 2 and 10 Gy for palliation (Fryer et al. 1978). Of these 245 patients, 44 developed radiation pneumonitis at a median time of 100 d post-exposure. The majority (>90%) of the patients developing radiation pneumonitis were treated with a ^{60}Co source to a midplane dose of either 8 Gy or 10 Gy. When accounting for the differences due to the ^{60}Co source (versus 6 MV photons in primates), the equivalent dose range at which pneumonitis was observed in the PBI/BM5 model approximate what has been reported in humans, and the latency to injury across that dose range is also similar (Van Dyk et al. 1981).

The MST for decedents in the PBI/BM5 model demonstrates a clear DRR. The MST is inversely related to the dose. This holds true considering all syndromes analyzed in the study, as well as for the subset of NHPs that survive beyond the latent period for lung injury

(e.g., NHPs that survive >60 d post-exposure). The incidence of radiation pneumonitis in the PBI/BM5 model appeared to increase as a function of dose up to a threshold of 11.0 Gy, above which it decreased. At 11.5 Gy and above, the prolonged GI mortality largely manifests prior to potentially lethal clinical pneumonitis causing the apparent incidence of clinical pneumonitis at these higher doses to appear lower. By comparison, in the WTLI model there is a clear dose-response relationship between incidence of pneumonitis and dose of exposure (Garofalo et al. [§§]). For example, the incidence of pneumonitis was 43% (3/7) following PBI/BM5 exposure in the dose range of 9.0–10.0 Gy versus an incidence of 39% (10/28) following WTLI exposure in the same dose range. However, following a PBI/BM5 exposure in the dose range of 11.0–11.5 Gy, the incidence of 50% (4/8) was well below the 94% (15/16) incidence following WTLI exposure in the same dose range. The difference in this dose range is predominantly due to the relatively low incidence (33%) following 11.5 Gy PBI/BM5 consequent to earlier prolonged GI syndrome mortality.

The spectrum of radiographic changes in the lung following radiation exposure was similar between the PBI/BM5 model and the WTLI model (Choi et al. 2004; Ikezoie et al. 1988; Libshitz and Shuman 1984). The predominant phenotypes for radiation-induced lung injury in the PBI/BM5 model were ground-glass opacities and consolidation, evolving later to traction bronchiectasis and scarring. In some cases, concomitant pulmonary effusions were seen, though these often resolved with dexamethasone treatment. The incidence and severity of radiation-induced lung injury as assessed by serial CT scan was dose-dependent during the period of time prior to supportive care treatment with dexamethasone (e.g., scans up to and including day 90 post-irradiation). Treatment with dexamethasone was generally effective as evidenced by reductions in respiratory rate and severity of radiographic injury. This is in keeping with that observed in humans. In a series of 17 patients treated with thoracic radiation and followed by serial CT scans, Ikezoe reported that 10 of 11 patients treated with steroids for pneumonitis had a reduced volume of injury on their subsequent CT scan (Ikezoie et al. 1988). Changes observed by CT scan and in NSRR following the latent period are influenced by treatment with steroids; thus steroid treatment needs to be standardized and controlled for in animal models of radiation-induced lung injury.

Corticosteroids are the standard of care treatment for radiation pneumonitis in the clinical setting and can be expected to be available and used in a mass casualty scenarios for the delayed lung syndrome (Berkely 2010). Given the latency to lung injury and the fact that the cytopenias associated with the H-ARS will have resolved by the time the lung syndrome manifests, there are no anticipated pragmatic barriers to treating victims with corticosteroids for radiation pneumonitis, and therefore they should be a part of medical management in the primate models of radiation-induced injury. Medical management has been demonstrated to increase the MST for ARS (Jackson et al. 1959; MacVittie et al. 1991; Perman et al. 1962;Bagdasarov et al. 1959; Thomas et al. 1962;MacVittie et al. 2005; Conard et al. 1956; Taketa 1962). Similarly, corticosteroid treatment was used in murine models of radiation-induced lung injury to influence survival and has been estimated to have a protection factor of 1.2 (Gross 1980; Gross et al. 1988; Libshitz and Shuman 1984). Comparable studies have not been performed in the NHP; therefore, the effect of corticosteroid treatment on survival and MST are unknown at this time. Durable reversal of potentially lethal radiation-induced pneumonitis through corticosteroid treatment may be possible following acute high-dose

exposure. Extended in vivo studies with and without corticosteroid support will be required to answer these and other questions.

The linkage to human organ-specific and multi-organ injury in the accident scenario: Radiation dose, severity and time course—The anecdotal data from multiple radiation accidents and that from several clinical databases provide a framework within which the human DRR for acute, potentially lethal irradiation subsyndromes can be formulated into the ARS and DEARE (Anno et al. 2003; Wiernik 1966a, b, c; MacVittie et al. 1996; Ricks and Fry 1990; Baranov et al. 1994; Van Dyk et al. 1981; Liu et al. 2008; Browne et al. 1990; Gourmelon et al. 2010; Hirama et al. 2003; Baranov 1996; Baranov and Guskova 1990; Guskova et al. 1990). The organ-specific and multi-organ sequelae of ARS and DEARE are linked by radiation-induced damage that occurs immediately and then progresses over a dose-dependent and organ-specific time course due to respective mechanisms of action and signs and symptoms that may be both overt and covert in action. There are several conclusions derived from radiation accident scenarios that are relevant to the development of animal models that can mimic the human radiation response and its treatment. These are: a) The radiation exposure environment is ill-defined; b) it is likely that all radiation exposures were nonuniform and heterogeneous therefore sparing a fraction of, or providing a dose differential to bone marrow, GI tissue, or lung; c) all radiation victims received supportive care of variable degree and timing, which was effective in enhancing survival time; d) MCM, if used, were administered at less than optimal schedules; and e) multiple organ injury will likely predominate over the time course of the DEARE following high dose exposures; e.g., >9.0 Gy. These data suggest that survivable doses of near uniform but heterogeneous radiation will be in the 9.0 to 12.0 Gy range with good supportive care and application of organ-specific or multi-organ effective MCM.

CONCLUSION

The DRR for the TBI-induced acute GI-ARS in NHPs receiving supportive care was recently determined (MacVittie et al. 2012). However, the TBI model, while providing the requisite DRR, prevents analysis of the full damage and recovery to the GI system since all animals would succumb to the subsequent 100% lethal H-ARS. Therefore, analysis of the long-term recovery of the GI system required development of a PBI model with minimal BM sparing. Furthermore, the threshold DRR for the GI-ARS and Lung-DEARE are approximate, and this model would provide the opportunity to analyze the coincident key sequelae of the ARS and DEARE; i.e., the acute GIARS, H-ARS, prolonged GI damage, and Lung-DEARE in a linked fashion. The model would also provide an opportunity to assess the long-term reconstitution of the hematopoietic system as well as that of severe thymic-derived naïve T-cell immunosuppression. In this regard, the model would mimic the human response to potentially lethal radiation exposure and treatment effects consequent to an accidental or terrorist nuclear event (Densow et al. 1997; MacVittie et al. 1996; Anno et al. 2003; Ricks and Fry 1990; Baranov et al. 1994;Meineke and Fliedner 2005; Liu et al. 2008; Konchalovsky et al. 2005; Konchalovsky 2010; Browne et al. 1990).

In summary, the PBI/BM5 NHP model that was developed:

- Provides the DRR for three key sequelae of the ARS and DEARE; the GI-ARS, H-ARS plus GI damage, and the lung DEARE. The DRR for the GI-ARS induced by the PBI/BM5 exposure resulted in an LD50/15 that is significantly different from that noted for the TBI-induced GI-ARS, although the respective slopes are not significantly different;

- Permits analysis of the full damage and recovery of the acute GI-ARS in the context of coincident H-ARS, continued multi-organ injury, and latent lung injury;

- Permits analysis of dose-dependent latency, incidence and severity of delayed lung injury in the context of coincident survival from acute and prolonged GI-ARS, H-ARS, and multi-organ injury;

- Permits analysis of the dose- and time-dependent incidence and severity of ARS and DEARE in a linked fashion, to include the potential effects of supportive care and that of organ-specific MCM;

- Permits analysis of the time course and natural history of coincident ARS and DEARE subsyndromes plus supportive care and treatment with MCM in the context a nuclear event;

- Permits analysis of MCM effects in a "reality scenario" of linked sequelae. It permits the analysis of the effects of 1) a single organ-specific MCM on the incidence and severity of other organ-specific sequelae and 2) the effects of combined MCM administration on all concomitant organ-specific sequelae;

- Permits determination of the effective schedule of administration of organ-specific MCM. The time interval for the efficacy of MCM for the H-ARS may well exceed the 24 to 72 h timeframe;

- Permits analysis of organ-specific biomarkers in a relevant radiation scenario of coincident subsyndromes and supportive care; and

- Can be modified to spare more or less BM to affect the severity of the ensuing H-ARS.

This animal model research platform, anchored by TBI models of H-ARS and GI-ARS and a WTLI model of lung injury characteristic of the DEARE, permits further understanding of the organ-specific damage that is survivable in a realistic nuclear scenario. The dose-dependent incidence, severity, and time relationships can be defined for each subsyndrome. Model refinement of the PBI/BM5 protocol permits assessment of the dose- and time-dependent sequelae in a linked fashion. It will provide invaluable insight into the mechanisms of action and the interactive and causal relationships between the ARS and DEARE. The research platform will provide essential information to interpret and define the complex interrelationships in clinically relevant models of the human radiation response to potentially lethal, near uniform irradiation and treatment.

Acknowledgments

Cassatt, Bert Maidment, Erika Lamb and Andrea Decarlo-Cohen, as well as the tremendous support and expertise of the research staff of the Preclinical Radiobiology Lab.

REFERENCES

Anno GH, Young RW, Bloom RM, Mercier JR. Dose response relationships for acute ionizing radiation lethality. Health Phys. 2003; 84:565–575. [PubMed: 12747475]

Bagdasarov AA, Raushenbakk MO, Abdullaev GM, Beliaeva BF, Lagutina NY. The treatment of acute radiation sickness with packed platelets. Probl Hematol Blood Transfus. 1959; 4:1–5.

Baltschukat K, Nothdurft W. Hematological effects of unilateral and bilateral exposures of dogs to 300-kVp x rays. Radiat Res. 1990; 123:7–16. [PubMed: 2371381]

Baranov, AE. Allogenic bone marrow transplantation after severe, uniform total-body irradiation: experience from recent (Nyasvizh, Belarus) and previous radiation accidents. In: MacVittie, TJ.; Weiss, JF.; Browne, D., editors. Advances in the treatment of radiation injuries: advances in the biosciences. Vol. 94. Tarrytown, NY: Pergamon; Elsevier Science Ltd; 1996. p. 281-293.

Baranov, AE.; Guskova, AK. Acute radiation disease in Chernobyl accident victims. In: Ricks, RC.; Fry, SA., editors. The medical basis for radiation accident preparedness II; clinical experience and follow-up since 1979. New York: Elsevier; 1990. p. 79-87.

Baranov AE, Selidovkin GD, Butturini A, Gale RP. Hematopoietic recovery after 10-Gy acute total body radiation. Blood. 1994; 83:596–599. [PubMed: 8286754]

Barker N, van Es JH, Kuipers J, Kujala P, van den Born M, Cozijnsen M, Haegebarth A, Korving J, Begthel H, Peters PJ, Clevers H. Identification of stem cells in small intesting and colon by marker gene Lg5. Nature. 2007; 449:1003–1007. [PubMed: 17934449]

Berkely FJ. Managing the adverse effects of radiation therapy. AM Fam Physician. 2010; 82:381–388. [PubMed: 20704169]

Bertho JM, Frick J, Prat M, Demarquay C, Dudoignon N, Trompier F, Gorin C, Thierry D, Gourmelon P. Comparison of autologous cell therapy and granulocyte colony-stimulating factor (G-CSF) injection vs. G-CSF alone for the treatment of acute radiation syndrome in a nonhuman primate model. Int J Radiat Oncol Biol Phys. 2005a; 63:911–920. [PubMed: 15913916]

Bertho JM, Prat M, Frick J, Demarquay C, Gaugler MH, Dudoignon N, Clairand I, Chapel A, Gorin NC, Thierry D. Application of autologous hematopoietic cell therapy to a nonhuman primate model of heterogeneous high-dose irradiation. Radiat Res. 2005b; 163:557–570. [PubMed: 15850418]

Bjerknes M, Cheng H. Clonal analysis of mouse intestinal epithelial progeitors. Gastroenterol. 1999; 116:7–14.

Bond VP, Robinson CV. A mortality determinant in nonuniform exposure of the mammal. Radiat Res. 1967; 7:265–275.

Bond VP, Carsten AL, Bullis J, Roth SP. Severity of organ injury as a predictor of acute mortality for disparate patterns of absorbed dose distribution. Radiat Res. 1991; 128:S9–S11. [PubMed: 1924756]

Broerse, JJ.; MacVittie, TJ., editors. Response of different species to total body irradiation. Boston: Martinus Nijhoff Publishers; 1984.

Bradford GB, Williams B, Rossi R, Bertoncello I. Quiescence, cycling, and turnover in the primitive hematopoietic stem cell compartment. Experimental Hematol. 1997; 25:445–453.

Browne D, Weiss JF, MacVittie TJ, Pillai MV. The first consensus development conference on the treatment of radiation injuries. International Journal of Radiation Biology. 1990; 57:437–442.

Calvi LM, Adams GB, Weibrecht KW, Weber JM, Olson DP, Knight MC, Martin RP, Schipani E, Divieti P, Bringhurst FR, Milner LA, Kronenberg HM, Scadden DT. Osteoblastic cells regulate the haematopoietic stem cell niche. Nature. 2003; 425:841–846. [PubMed: 14574413]

Carbonneau CL, Despars G, Rojas-Sutterlin S, Fortin A, Le O, Hoang T, Beausejour CM. Ionizing radiation-induced expression of INK4a/ARF in murine bone marrow-derived stromal cell populations interferes with bone marrow homeostasis. Blood. 2012; 119:717–726. [PubMed: 22101896]

Cheng H, Leblond CP. Origin, differentiation, and renewal of four main epithelial cell tyoes in the mouse small intestine: V. Unitarian theory of the origin of the four epithelial cells types. Am J Anat. 1974; 141:537–561. [PubMed: 4440635]

Cheshier SH, Morrison SJ, Liao X, Weissman IL. In vivo proliferation and cell cycle kinetics of long-term self-renewing hematopoietic stem cells. Proc Natl Acad Sci. 1999; 96:3120–3125. [PubMed: 10077647]

Choi YW, Munden RF, Erasmus JJ, Park KF, Chung WK, Jeon SC, Park CK. Effects of radiation therapy on the lung: radiologic appearances and differential diagnosis. Radiographics. 2004; 24:985–997. [PubMed: 15256622]

Cole LJ, Haire HM, Alpen EL. Partial shielding of dogs: effectiveness of small external epicondylar lead cuffs against lethal x-radiation. Radiat Res. 1967; 32:54–63. [PubMed: 6053865]

Conard RA, Cronkite EP, Brecher G, Strome CPA. Experimental therapy of the gastrointestinal syndrome produced by lethal doses of ionizing radiation. J Applied Physiol. 1956; 9:227–233. [PubMed: 13376434]

Densow D, Kindler H, Baranov AE, Tibken B, Hofer EP, Fliedner TM. Criteria for the selection of radiation accident victims for stem cell transplantation. Stem Cells. 1997; 15(Suppl 2):287–297. [PubMed: 9368315]

Dominici M, Rasini V, Bussolari R, Chen X, Hofmann TJ, Spano C, Bernabei D, Veronesi E, Bertoni F, Paolucci P, Conte P, Horwitz EM. Restoration and reversible expansion of the osteoblastic hematpoietic stem cell niche after marrow radioablation. Blood. 2009; 114:2333–2343. [PubMed: 19433859]

Down JD, Steel GG. The expression of early and late damage after thoracic irradiation: a comparison between CBA and C57B1 mice. Radiat Res. 1983; 96:603–610. [PubMed: 6657925]

Farese AM, Cohen MV, Katz BP, Smith CP, Jackson W III, Cohen DM, MacVittie TJ. A nonhuman primate model of the hematopoietic acute radiation syndrome plus medical management. Health Phys. 2012; 103(4):367–382. [PubMed: 22929469]

Finney, DJ. Probit analysis. Cambridge, UK: Cambridge University Press; 1947.

Fliedner TM, Graessle D, Meineke V, Dorr H. Pathophysiological principles underlying the blood cell concentration responses used to assess the severity of effect after accidental whole-body radiation exposure: an essential basis for evidence-based clinical triage. Exp Hematol. 2007; 35:8–16. [PubMed: 17379081]

Franko AJ. The genetic basis of strain-dependent differences in the early phase of radiation injury in mouse lung. Radiat Res. 2010; 126:349–356. [PubMed: 1852022]

Fryer CJHFPJ, Rider WD, Poon P. Radiation pneumonitis: experience following a large single dose of radiation. Int J Radiat Oncol Biol Phys. 1978; 4:931–936. [PubMed: 721655]

Gourmelon P, Benderitter M, Bertho J-M, Gorin NC, De Revel P. European consensus on the medical management of acute radiation syndrome and analysis of the radiation accidents in Belgium and Senegal. Health Phys. 2010; 98:825–832. [PubMed: 20445389]

Gross NJ. Radiation pneumonitis in mice. Some effects of corticosteroids on morality and pulmonary physiology. J Clin Invest. 1980; 66:504–510. [PubMed: 7400326]

Gross NJ, Narine KR, Wade R. Protective effect of corticosteroids on radiation pneumonitis in mice. Radiat Res. 1988; 113:112–119. [PubMed: 3340715]

Guskova, AK.; Nadezhina, NM.; Barabanova, AV.; Baranov, AE.; Gusev, IA.; Protasova, TG.; Boguslavskij, VB.; Pokrovskaya, VN. Acute effects of radiation exposure following the Chernobyl accident, immediate results of radiation sickness and outcome of treatment. In: Browne, D.; Weiss, JF.; MacVittie, TJ.; Pillai, MV., editors. Treatment of radiation injuries. New York: Plenum Press; 1990. p. 195-209.

Handford SW, Johnson PW, Scholtes RJ, Duny MS. The small intestine in acute radiation death in the dog. Radiat Res. 1961; 15:734–744. [PubMed: 13904307]

Hansen CL, Michaelson SM, Howland SW. Lethality of upper body exposure in beagles. Health Phys. 1961; 76:242–246.

Hill RP. Radiation effects on the respiratory system. Brit J Radiol. 2005; 27:81.

Hirama T, Tanosaki S, Kandatsu S, Kuroiwa N, Kamada T, Tsuji H, Tamada S, Katoh H, Yamamoto N, Tsuji H, Suzuki G, Akashi M. Initial medical management of patients severely irradiated in the Tokai-mura criticality accident. Brit J Radiol. 2003; 76:246–253. [PubMed: 12711644]

Igaki H, Kakagawa K, Uozaki H, Akahane M, Hosoi Y, Fukayama K, Miyagawa K, Akashi M, Ohtomo K, Maekawa K. Pathological changes in the gastrointestinal tract of a heavily radiation-exposed worker at the Tokai-mura criticality accident. J Radiat Res. 2008; 49:55–62. [PubMed: 17938558]

Ikezoie J, Takashima S, Morimoto S, Kadowaki K, Takeuchi N, Yamamoto T, Nakanishi K, Isaza M, Arisawa J, Ikeda H, Masaki N, Kozuka T. CT appearance of acute radiation-induced injury in the lung. AJR AM J Roentgenol. 1988; 150:765–770. [PubMed: 3258086]

Jackson DP, Sorensen DK, Cronkite EP, Bond VP, Fliedner TM. Effectiveness of transfusions of fresh and lyophiloized platelets in controlling bleeding due to thrombocytopenia. J Clinical Investigation. 1959; 38:1689–1697.

Jang Y-Y, Sharkis SJ. A low level of reactive oxygen species selects for primitive hematopoietic stem cells that may reside in the low-oxygenic niche. Blood. 2007; 110:3056–3063. [PubMed: 17595331]

Kim T-H, Escudero S, Shivdasani RA. Intact function of Lgr5 receptor-expressing intestinal stem cells in the absence of paneth cells. PNAS. 2012; 109:3932–3937. [PubMed: 22355124]

Konchalovsky MV, Baranov AE, Kolganov AV. Multiple organ involvment and failure: selected Russian radiation accident cases re-visited. Br J Radiol. 2005; 78:26–29.

Konchalovsky MV. Multiple organ involvement and failure: selected Russian radiation accident cases re-visited. BJR Supplement/BIR. 2010; 27:26–29. [PubMed: 15975868]

Liao ZX, Travis EL, Tucker SL. Damage and morbidity from pneumonitis after irradiation of partial volumes of mouse lung. Int J Radiat Oncol Biol Phys. 1995; 32:1359–1370. [PubMed: 7635776]

Libshitz HI, Shuman LS. Radiation-induced pulmonary change: CT findings. J Comput Assit Tomogr. 1984; 8:15–19.

Liu Q, Jiang B, Jiang L-P, Wu Y, Wang X-G, Zhao F-L, Fu B-H, Turai I, Jiang E. Clinical report of three cases of acute radiation sickness from a ^{60}Co radiation accident in Henan province in China. J Radiat Res. 2008; 49:63–69. [PubMed: 18187937]

MacVittie TJ, Monroy R, Vigneulle RM, Zeman GH, Jackson WE. The relative biological effectiveness of mixed fission-neutron: gamma radiation on the hematopoietic syndrome in the canine: effect of therapy on survival. Radiat Res. 1991; 128:S29–S36. [PubMed: 1924744]

MacVittie, TJ.; Weiss, JF.; Browne, D. Consensus summary on the treatment of radiation injuries. In: MacVittie, TJ.; Weiss, JF.; Browne, D., editors. Advances in the treatment of radiation injuries. Tarrytown, NY: Pergamon, Elsevier Sciences Inc.; 1996. p. 325-346.

MacVittie TJ, Farese AM, Jackson WI. Defining the full therapeutic potential of recombinant growth factors in the post radiation-accident environment: the effect of supportive care plus administration of G-CSF. Health Phys. 2005; 89:546–555. [PubMed: 16217198]

MacVittie TJ, Farese AM, Bennett A, Gelfond D, Shea-Donohue T, Tudor G, Booth C, McFarland E, Jackson W III. The acute gastrointestinal subsyndrome of the acute radiation syndrome: a Rhesus macaque model. Health Phys. 2012; 103(4):411–426. [PubMed: 22929470]

Mahmud N, Devine SM, Weller KP, Parmar S, Sturgeon C, Nelson MC, Hewett T, Hoffman R. The relative quiescence of hematopoietic stem cells in nonhuman primates. Blood. 2001; 97:3061–3068. [PubMed: 11342431]

Maillie HD, Krasavage W, Mermagen H. On the partial body irradiation of the dog. Health Phys. 1966; 12:883–887. [PubMed: 5956203]

Marks LB, Yu X, Vujaskovic Z, Small W Jr, Folz R, Anscher MS. Radiation-induced lung injury. Semin Radiat Oncol. 2003; 13:333–345. [PubMed: 12903021]

Mason KA, Withers HR, McBride WH, Davis CA, Smathers JB. Comparison of the gastrointestinal syndrome after total-body or total-abdominal irradiation. Radiat Res. 1989; 117:480–488. [PubMed: 2648450]

Meineke V, Fliedner TM. Radiation-induced multi-organ involvement and failure: challenges for radiation accident medical management and future research. Br J Radiol. 2005; 27(Suppl):196–200.

Monroy RL, Skelly RR, Taylor P, Dubois A, Donahue RE, MacVittie TJ. Recovery from severe hemopoietic suppression using recombinant human granulocyte-macrophage colony stimulating factor. Experimental Hematol. 1988; 16:334–338.

Morrison SJ, Spradling AC. Stem cells and niches: mechanisms that promote stem cell maintenanace throughout life. Cell. 2008; 132:598–611. [PubMed: 18295578]

Newcomb CH, Van Dyk J, Hill RP. Evaluation of isoeffect formulae for predicting radiation-induced lung damage. Radiother Oncol. 1993; 26:51–63. [PubMed: 8438087]

Perman V, Cronkite EP, Bond VP, Sorensen DK. The regenerative ability of hemopoietic tissue following lethal x-irradiation in dogs. Blood. 1962; 19:724–737. [PubMed: 14485433]

Potten CS. Continuous labeling studies on mouse skin and intestine. Cell Tissue Kinet. 1974; 7:271–283. [PubMed: 4837676]

Potten CS. Extreme sensitivity of some intestinal crypt cells to X irradiation. Nature. 1977; 269:518–521. [PubMed: 909602]

Potten CS, Rezvani M, Hendry JH, Moore JV, Major D. Correction of intestinal microcolony counts for variation in size. Int J Radiat Biol Relat Stud Phys Chem Med. 1981; 40:321–326. [PubMed: 7026475]

Rauchwerger M. Radiation protection by tibia-shielding in adult, weanling and suckling mice. Int J Radiat Biol. 1972; 22:269–278.

Ricks, RC.; Fry, SA., editors. The medical basis for radiation accident preparedness II: clinical experience and follow-up since 1979. New York: Elsevier; 1990.

Sangiorgi E, Capecchi MR. Bmi 1 is expressed in vivo in intestinal stem cells. Nat Genet. 2008; 40:915–920. [PubMed: 18536716]

Scadden DT. The stem-cell niche as an entity of action. Nature. 2006; 441:1075–1079. [PubMed: 16810242]

Taketa ST. Water-electrolyte and antibiotic therapy against acute (3 to 5 day) intestinal radiation death in the rat. Radiat Res. 1962; 16:312–326. [PubMed: 13919239]

Taketa TS, Swift MN, Bond VP. Modification of radiation injury in rats through gastrointestinal tract shielding and bone marrow therapy. Am J Physiol. 1959; 196:987–992. [PubMed: 13649915]

Taketa ST, Carsten AL, Cohn SH, Atkins HL, Bond VP. Active bone marrow distribution in the monkey. Life Sci. 1970; 9:169–174. [PubMed: 4985006]

Terry NH, Travis EL. The influence of bone marrow depletion on intestinal radiation damage. International J Radiat Oncol Biol Phys. 1989; 17:569–573.

Thomas ED, Collins JA, Herman EC Jr, Ferrebee JW. Marrow transplants in lethally irradiated dogs given methotrexate. Blood. 1962; 19:217–228. [PubMed: 13920766]

Tian H, Biehs B, Warming S, Leong KG, Rangell L, Klein OD, de Sauvage FJ. A reserve stem cell population in small intestine renders Lgr5-positive cells dispensable. Nature. 2011; 478:255–260. [PubMed: 21927002]

Traycoff CM, Orazi A, Ladd AC, Rice S, McMahel J, Srour EF. Proliferation-induced decline of primative hematopoietic progenitor cell activity is coupled with an increase in apoptosis in ex vivo expanded CD34+ cells. Experimental Hematol. 1998; 26:53–62.

van Bekkum DW. Radiation sensitivity of the hemopoietic stem cell. Radiat Res. 1991; 128:S4–S8. [PubMed: 1924746]

Van Dyk J, Keane TJ, Kan S, Rider WD, Fryer CJ. Radiation pneumonitis following large single dose irradiation: a reevaluation based on absolute dose to lung. Int J Radiat Oncol Biol Phys. 1981; 7:461–467. [PubMed: 7251416]

Vriesendorp HM, Vigneulle RM, Kitto G, Pelky T, Taylor P, Smith J. Survival after total body irradiation: effects of irradiation of exteriorized small intestine. Radiotherapy Oncol. 1992; 23:160–169.

Wang J, Wang B, Chen D, Luo Y. The response of dogs to mixed neutron-g radiation with different n/g ratios. Radiat Res. 1991; 128:S42–S46. [PubMed: 1924747]

Wang Y, Liu L, Pazhanisamy SK, Li H, Meng A, Zhou D. Total body irradiation causes residual bone marrow injury by induction of persistent oxidative stress in murine hematopoietic stem cells. Free Radical Biol Medicine. 2010; 48:348–356.

Wiernik G. Changes in the villous pattern of the human jejunum associated with heavy radiation damage. Gut. 1966a; 7:149–153. [PubMed: 5932892]

Wiernik G. In-vivo cell kinetics of a normal human tissue. Brit Med J. 1966b; 2:385–387. [PubMed: 5917357]

Wiernik G. Radiation damage and repair in the human jejunal mucosa. J Pathol. 1966c; 91:389–393.

Yan KS, Chia LA, Li X, Ootani A, Su J, Lee JY, Su N, Luo Y, Heilshorn SC, Amieva MR, Sangiorgi E, Capecchi MR, Kuo CJ. The intestinal stem cell markers Bmi1 and Lgr5 identify two functionally distinct populations. PNAS. 2012; 109:466–471. [PubMed: 22190486]
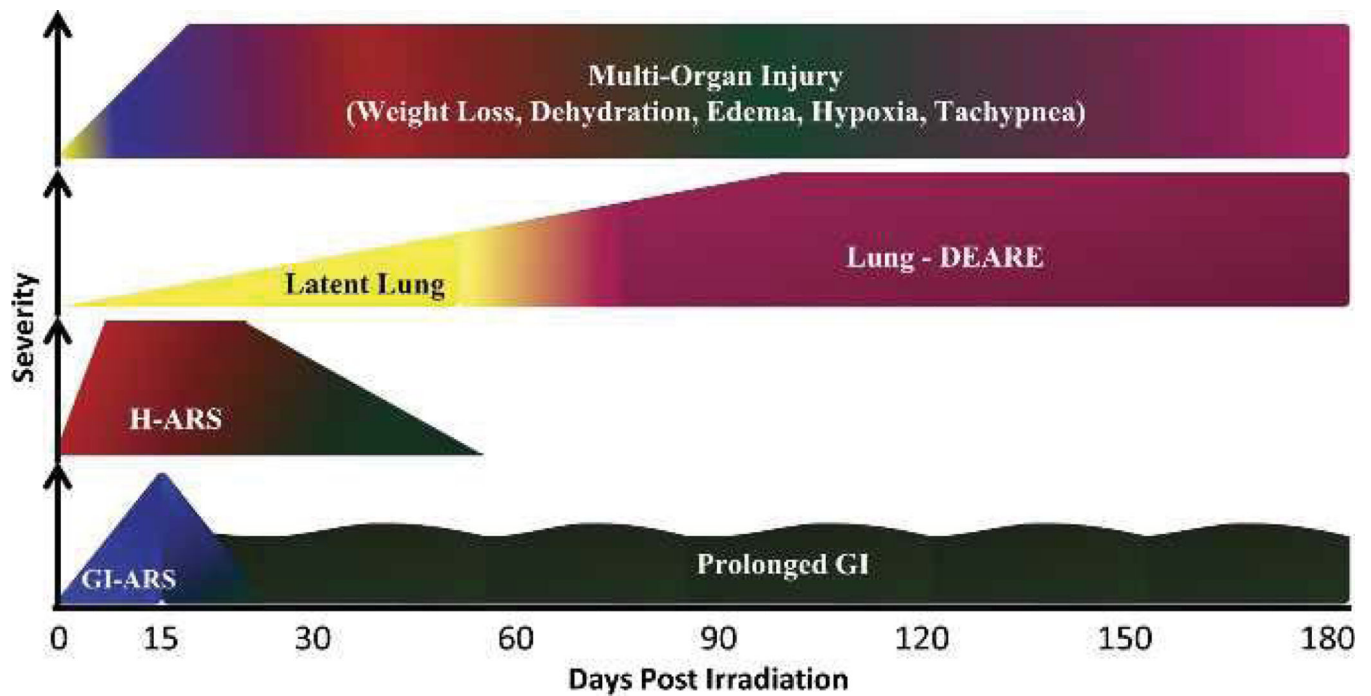
Fig. 1.
Time course and severity of multiple organ injury following PBI/BM5. Exposure to
PBI/BM5 results in the expression of key sequelae of ARS and DEARE, to include the acute
GI-ARS, H-ARS with coincident prolonged GI damage, continued prolonged GI damage,
lung injury, and multi-organ injury through 180 d post-exposure.
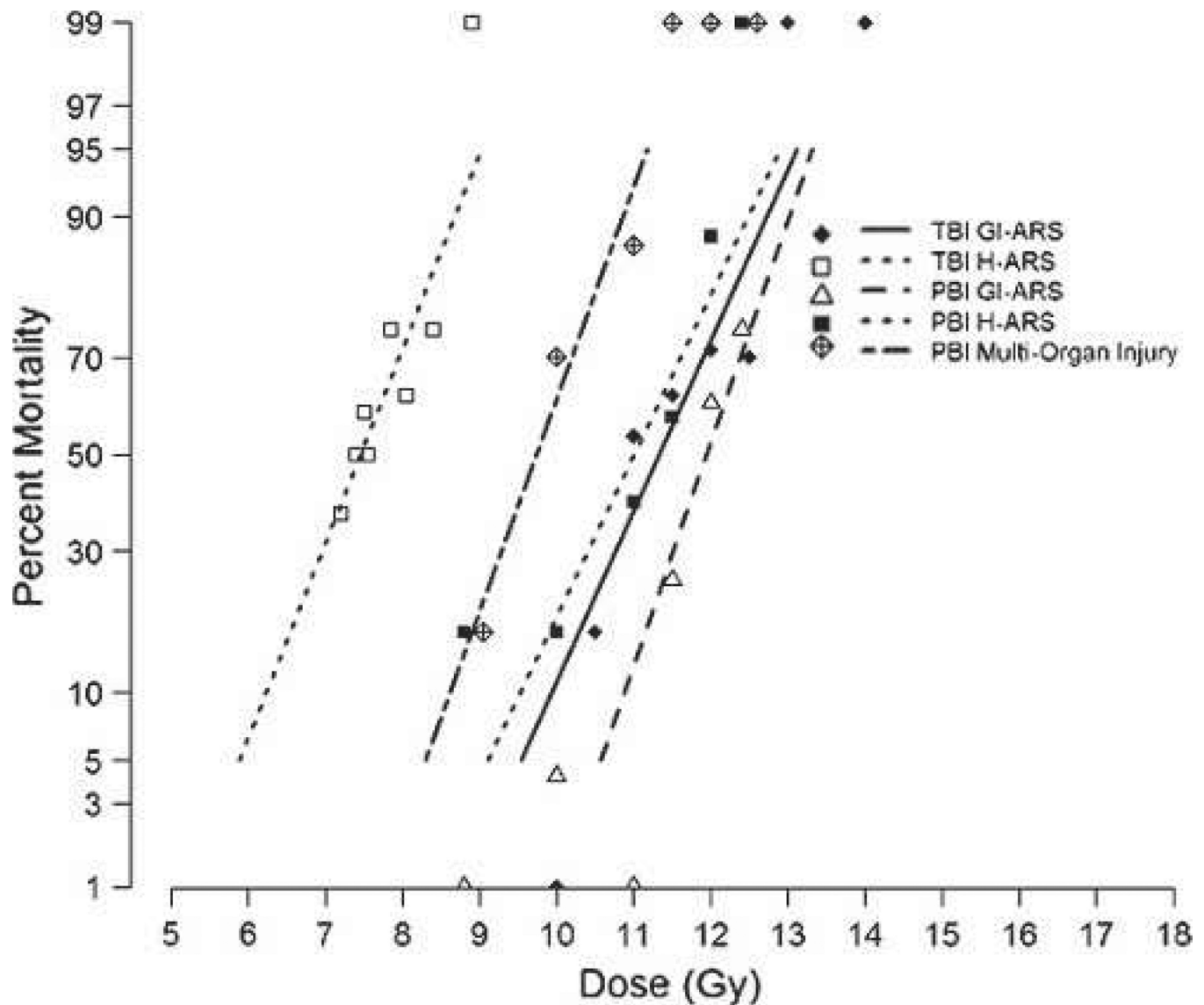
Fig. 2.
DRR for ARS and DEARE due to TBI and PBI/BM5 of rhesus macaques. Rhesus macaques were exposed to TBI or PBI/BM5 using 6MV LINAC-derived photons at a dose rate of 0.80 Gy min^{-1}. Irradiations and animal care for each DRR were performed at the same radiation and veterinary facilities with the same research team (Farese et al. 2012; MacVittie et al. 2012). All exposures were measured as midline tissue dose. The DRRs were defined over time frames to assess organ-specific subsyndromes (15 and 60 d for GI-ARS and H-ARS, respectively) or multi-organ syndromes (180 d).
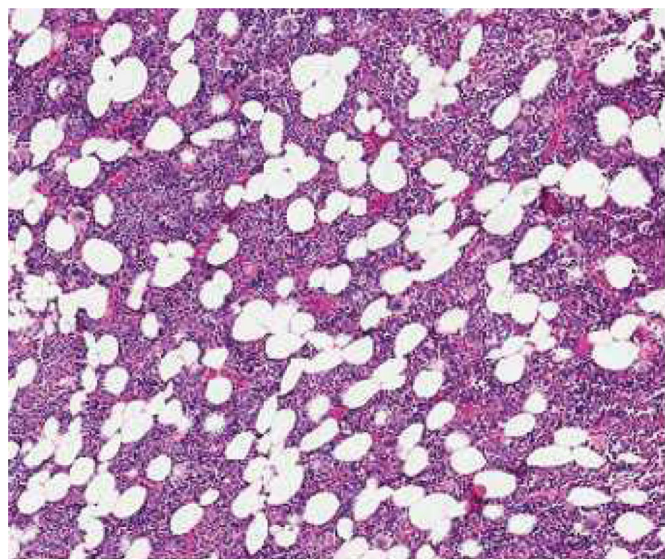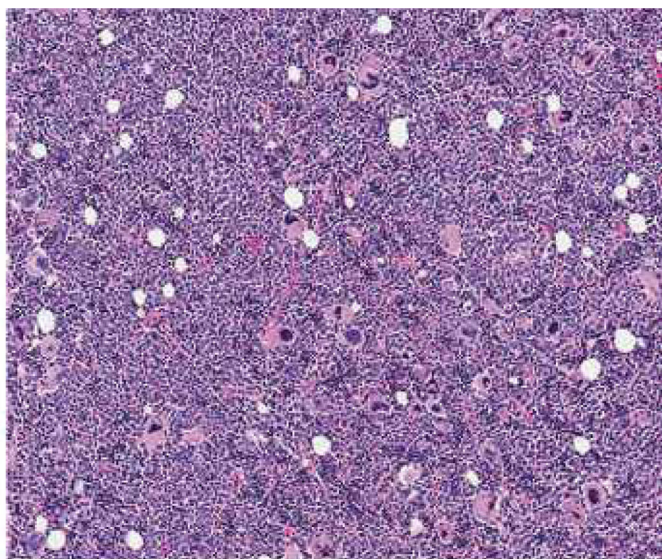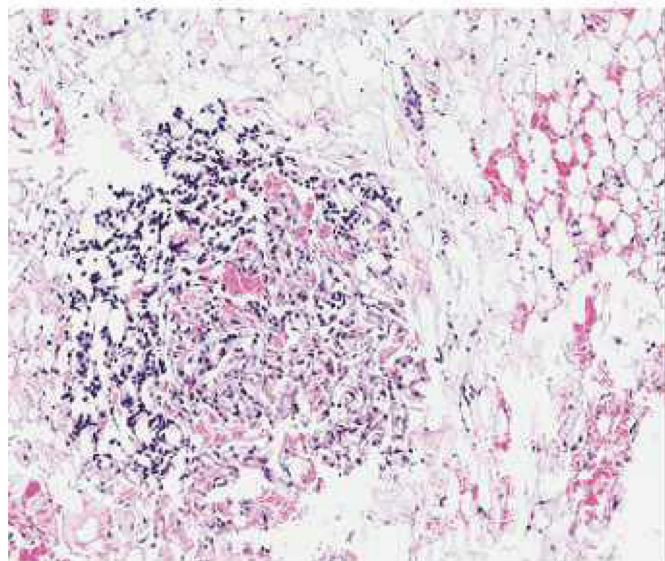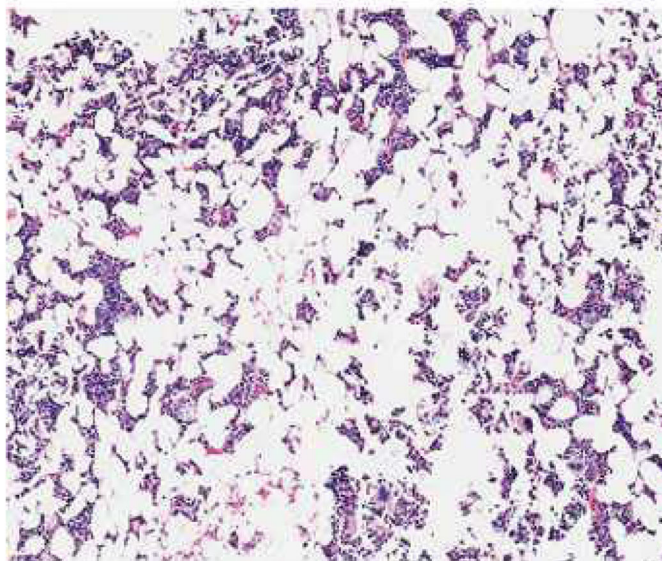
Fig. 3.
Histology of irradiated and spared bone marrow in rhesus macaques exposed to PBI/BM5.
Bone marrow samples were procured from the tibia and femur. In vivo dosimetry was used
to estimate the dose received to the tibiae and midline of each animal as described in
Materials and Methods. The average dose to surface of tibiae was 0.53 Gy across all doses
(9.0–12.5 Gy PBI) delivered to the animals. Representative photographs were taken at 10×
magnification. Samples were stained with H&E.
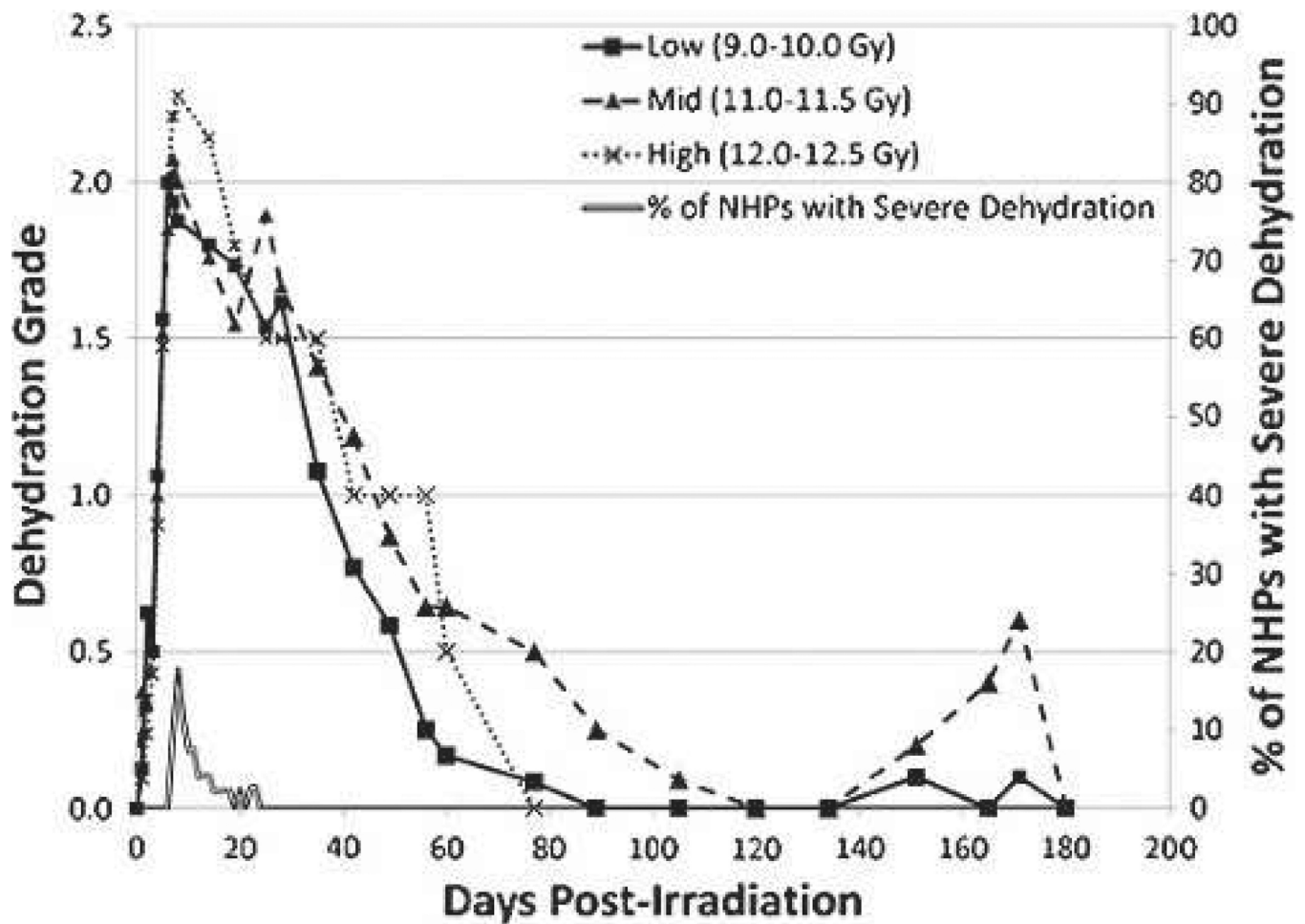
Fig. 4.
Dehydration over time in rhesus macaques exposed to PBI/BM5. The grade of hydration and
% of NHPs with severe dehydration versus time (d) post-PBI/BM5. Mean values are plotted
for NHPs grouped into Low (9.0–10.0 Gy), Mid (11.0–11.5 Gy), and High (12.0–12.5 Gy)
dose cohorts. Grades for dehydration were (0) for normal hydration, (1) for mild
dehydration, (2) for moderate dehydration, and (3) for severe dehydration. Hydration status
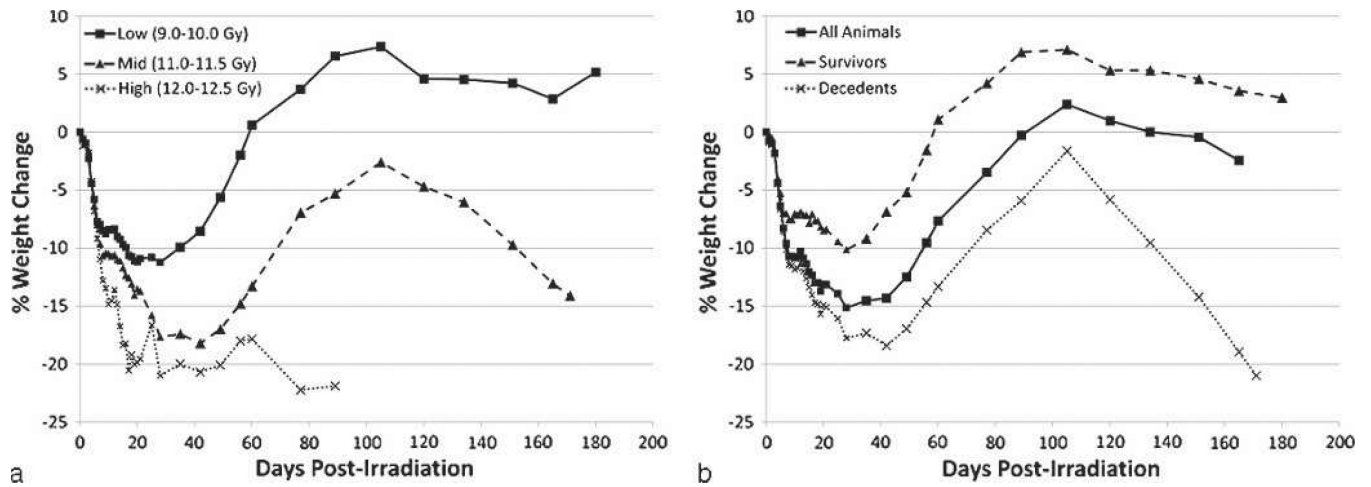was evaluated daily.

Fig. 5.
Weight loss over time in rhesus macaques exposed to PBI/BM5. The % weight change relative to pre-irradiation body weight versus time (d) post-irradiation. Mean values are plotted for (a) NHPs grouped into dose cohorts, and (b) all studied NHPs, survivors, and decedents. Animals were weighed daily.
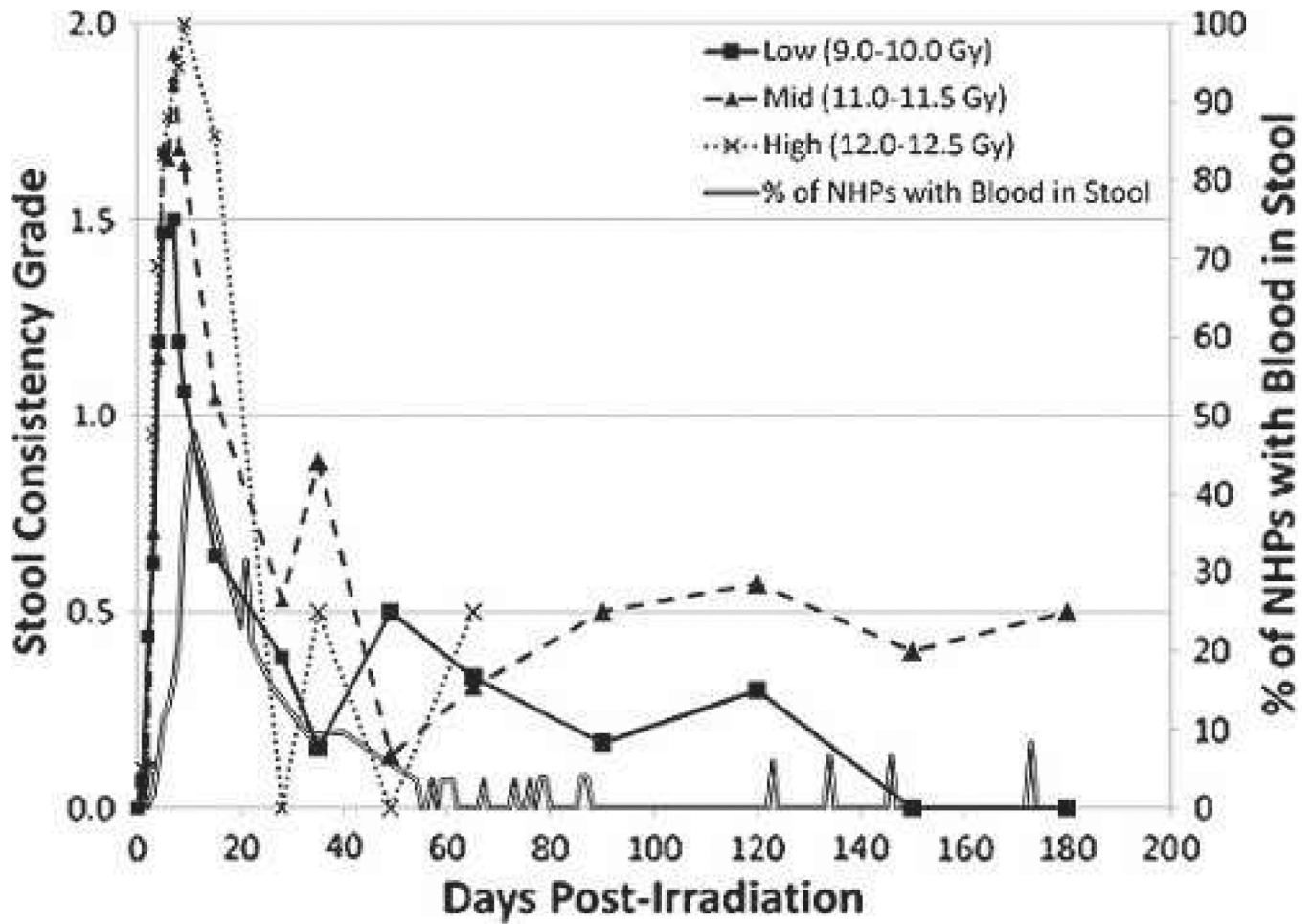
Fig. 6.
Diarrhea over time in rhesus macaques exposed to PBI/BM5. The severity and duration of diarrhea, assessed as grade of stool consistency and % of NHPs with bloody stool, versus time (days) post-irradiation. Mean values are plotted for NHPs grouped into dose cohorts. Each animal's stool consistency was monitored twice a day for the duration of the in vivo phase of the study. The presence of blood in stool was evaluated concurrently. Stool grades were (0) for formed stool, (1) for soft stool, and (2) for diarrhea.
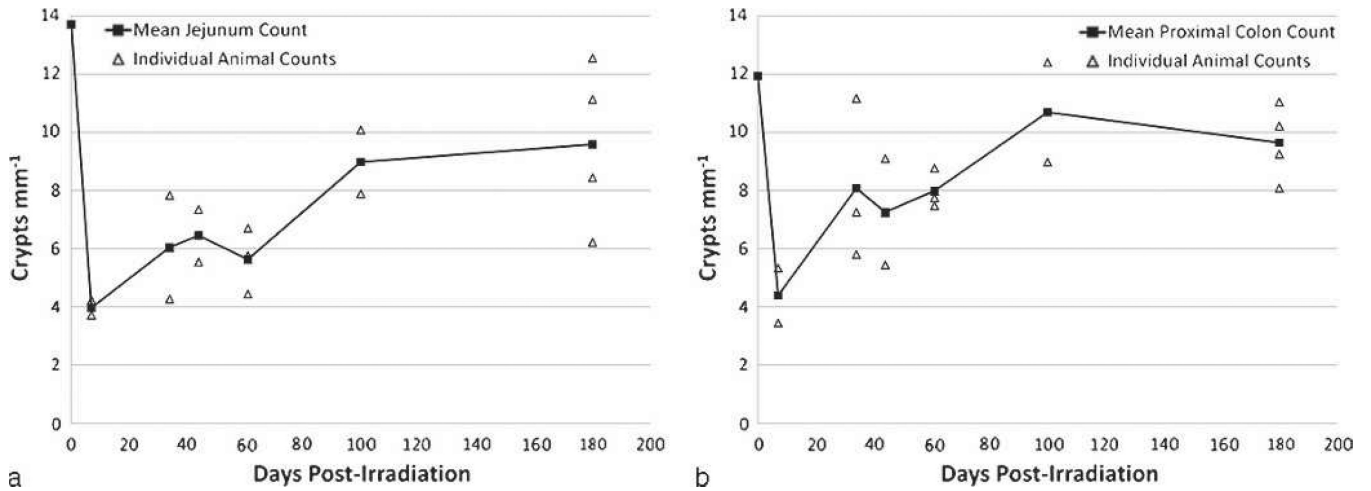
Fig. 7.
Radiation-induced loss and recovery of crypts in the jejunum and proximal colon of rhesus macaques exposed to PBI/BM5. Crypts were counted in the jejunum (a) and proximal colon (b) of animals exposed to 10.0 Gy PBI/BM5. Tissue was procured at days 7, 34, 44, 61, 100, and 180 post-exposure. Tissues were fixed in formalin, sectioned, and stained with H&E. A correction factor was applied to correct for error due to variation in crypt width, as detailed in Materials and Methods. The mean values are plotted with the values for each individual animal that was analyzed. The day 0 values are means from counts performed on non-irradiated, normal NHPs ($n = 10$).
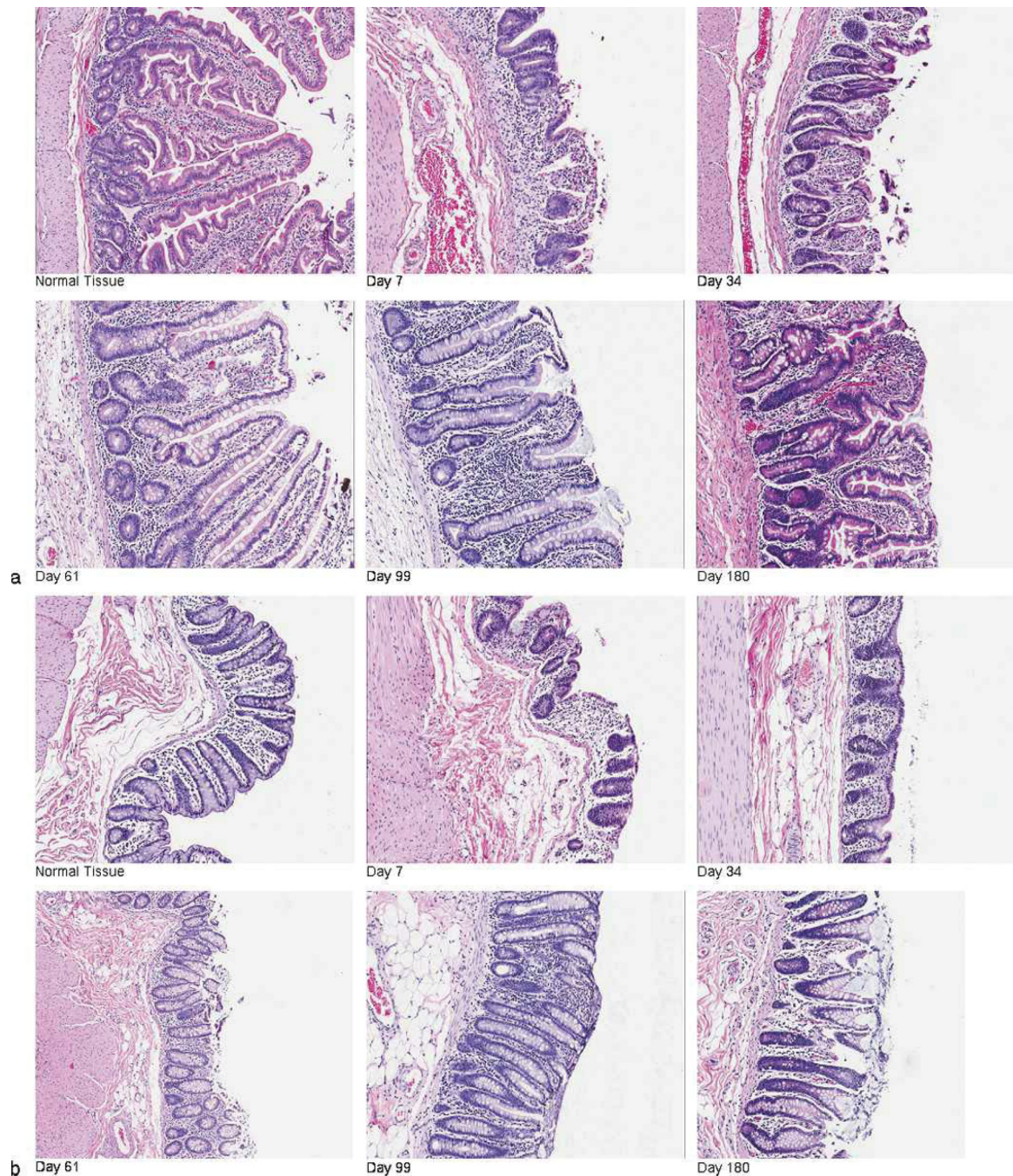
Fig. 8.
Radiation-induced GI damage and recovery in rhesus macaques exposed to PBI/BM5. Animals were exposed to 10.0 Gy PBI/BM5. Tissue was procured from (a) the jejunum and (b) proximal colon at necropsy on selected study days (days 7, 44, 62, 100, and 180) across the 180 day in vivo time course. Tissue was fixed in formalin, sectioned, and stained with H&E. Representative photographs show the loss and disorganized regeneration of crypts and villi over time post-PBI/BM5. All photographs were taken at 10× magnification.
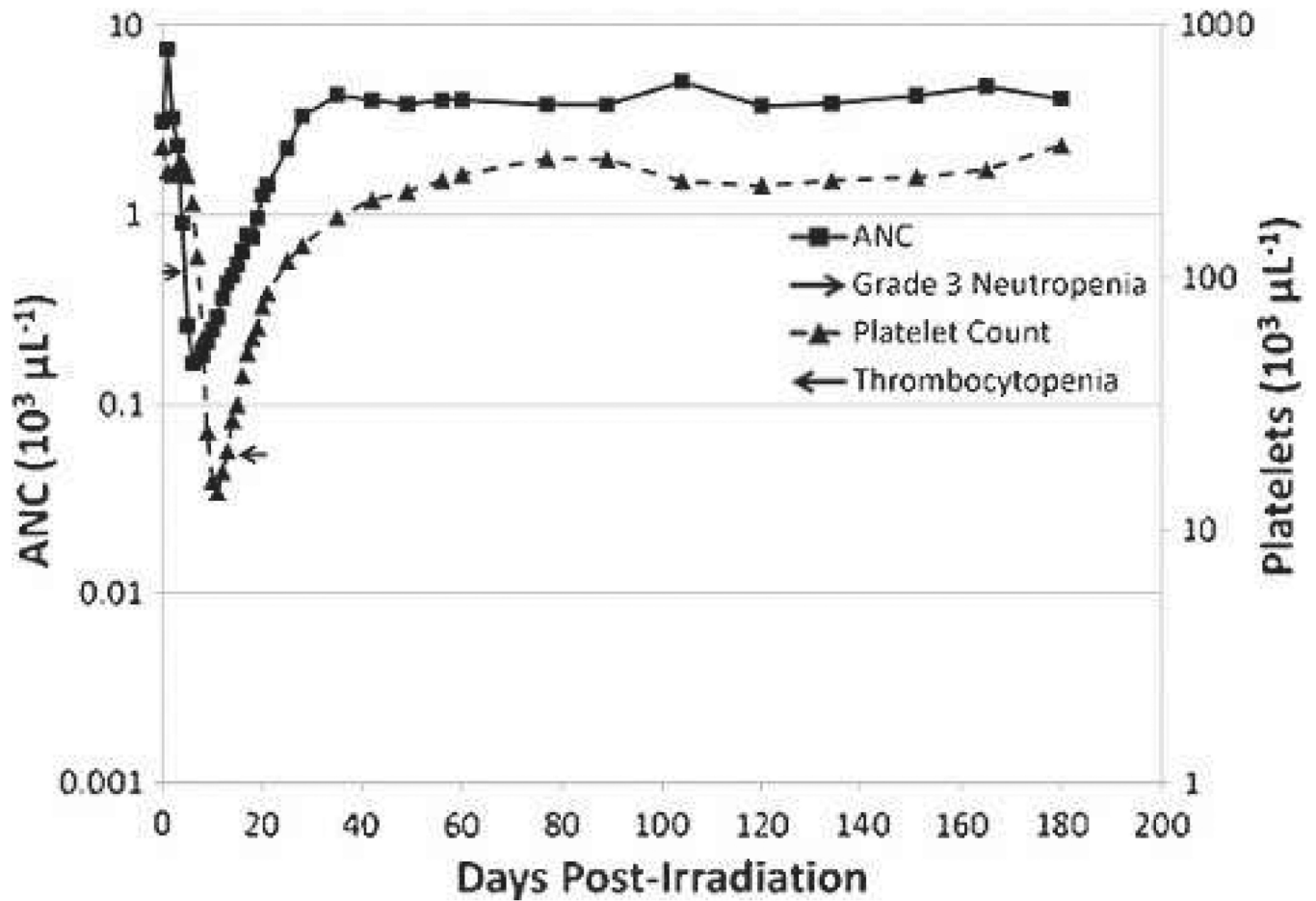
Fig. 9.
The time course of neutropenia and thrombocytopenia in rhesus macaques exposed to PBI/
BM5. Mean values are plotted for ANC and platelet counts over time in days post-
irradiation. Grade 3 neutropenia is defined as ANC ≤ 500 μL^{-1}, and thrombocytopenia is
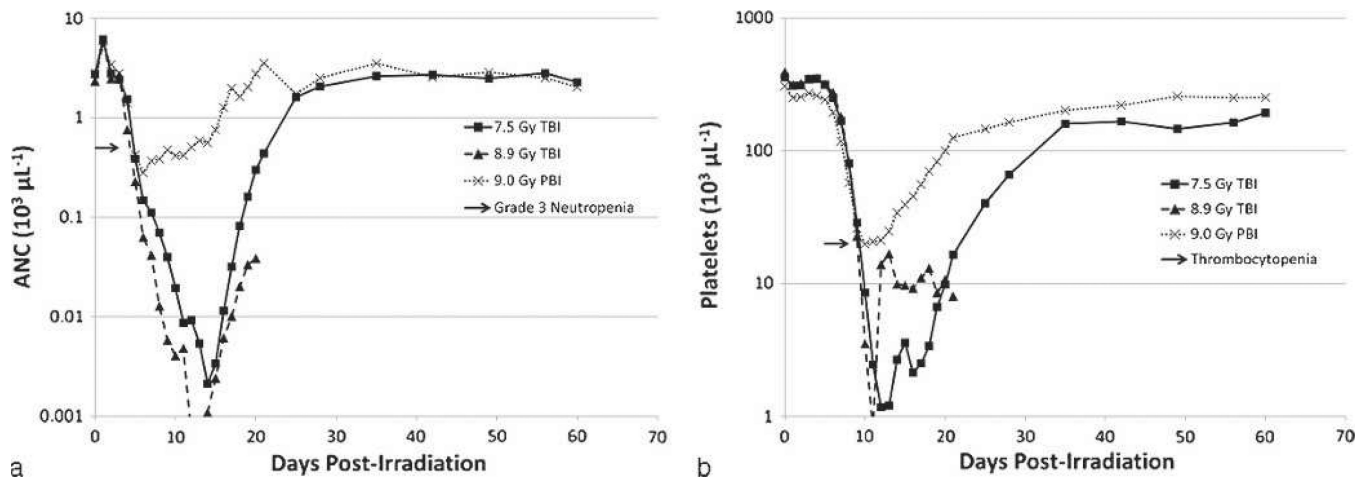defined as platelets <20,000 μl^{-1}.

Fig. 10.
Comparison of the time course of neutropenia and thrombocytopenia in rhesus macaques exposed to PBI/BM5 or TBI. NHPs were exposed to TBI or PBI/BM5 using 6 MV LINAC-derived photons at 0.80 Gy min^{-1}. The 9.0 Gy PBI/BM5 exposure is estimated to be an approximate LD50/60, whereas TBI at 8.9 Gy or 7.5 Gy are LD100/60 and LD50/60 doses, respectively. Mean values are plotted for (a) ANC and (b) platelet counts over time post-irradiation.
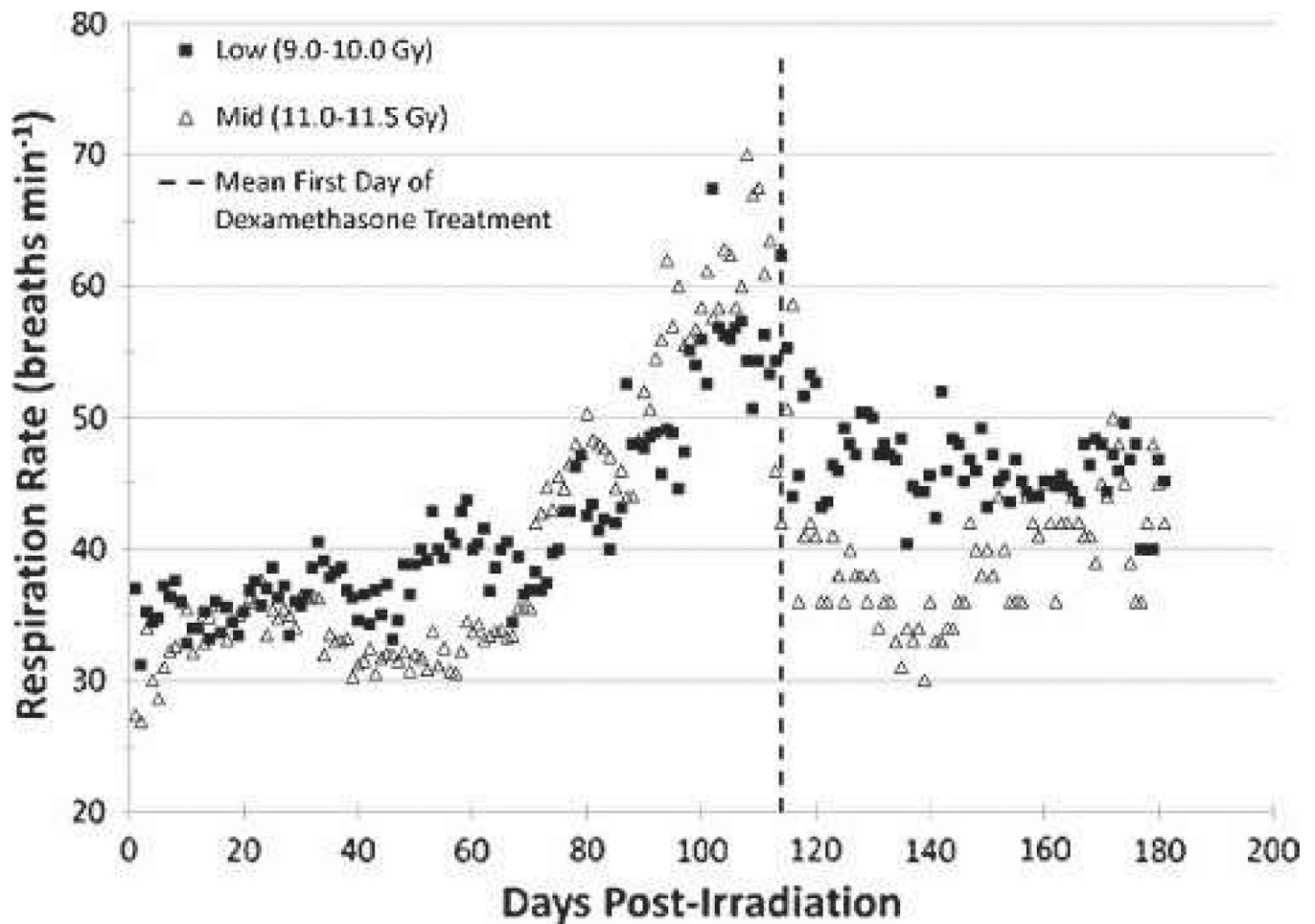
Fig. 11.
Respiratory rate in rhesus macaques exposed to PBI/BM5. Changes in mean NSRR are plotted as a function of time post-irradiation. This analysis was restricted to NHPs that survived >60 d post-exposure (e.g., survivors of GI-ARS and H-ARS coincident with prolonged GI; $n = 28$) and for whom serial daily NSRR data were available ($n = 15/28$). Mean values are plotted for NHPs grouped into dose cohorts. Animals in the High (12.0–12.5 Gy) dose cohort are not shown as only two of those NHPs survived >60 d, neither of which had serial NSRR data. The mean time to initiation of dexamethasone supportive care treatment was 114 d post-exposure for all NHPs on the plot.
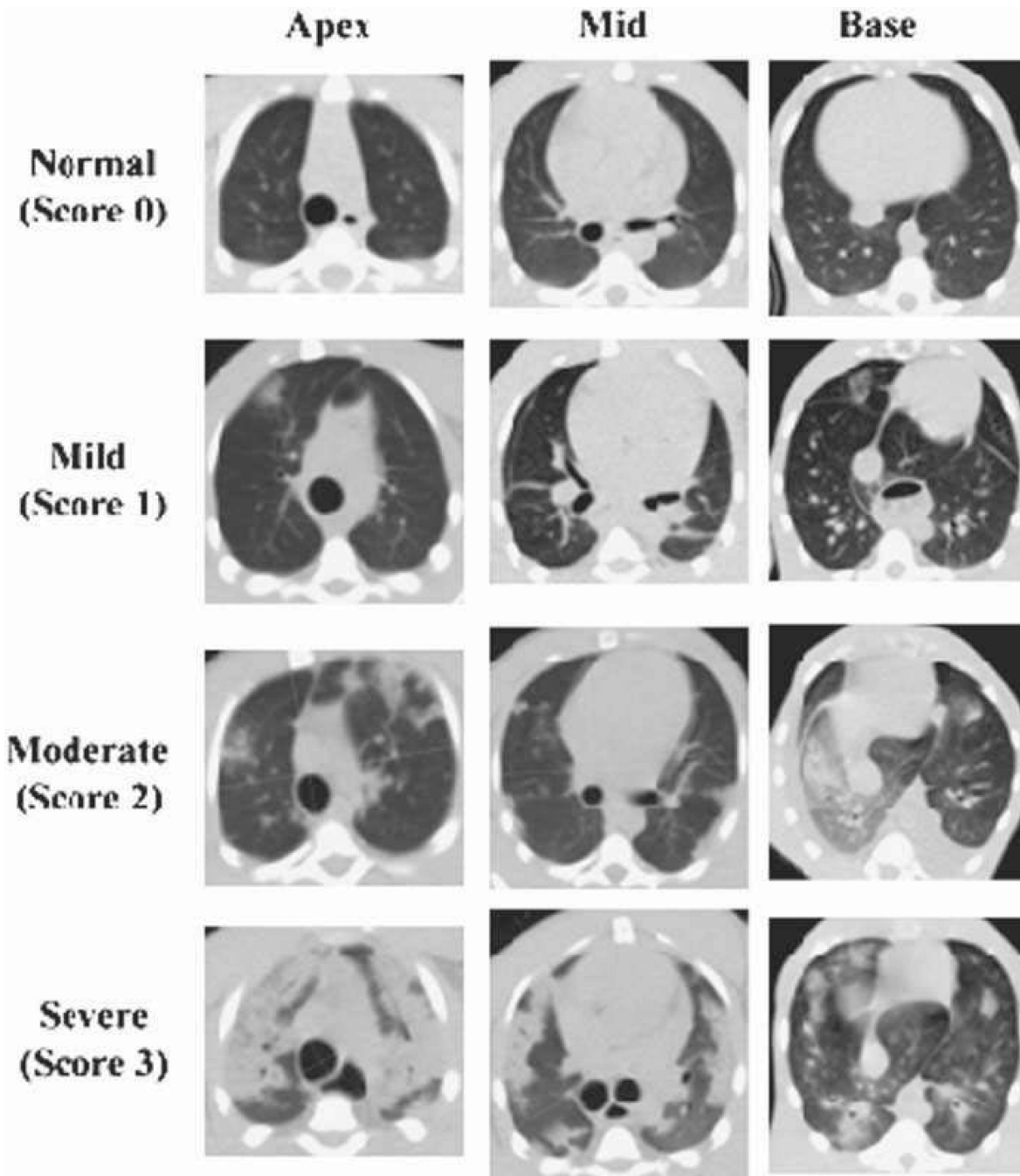
Fig. 12.
Radiographic severity scoring of pulmonary injury in rhesus macaques exposed to PBI/ BM5. Representative images characteristic of the qualitative scoring of radiation-induced lung injury are shown. CT images were assessed for evidence of radiation-induced lung injury (pneumonitis and fibrosis) based on characteristic changes in radiodensity. All CT scans were assessed by a radiation oncologist with expertise in thoracic radiography and scored as mild (1), moderate (2), or severe (3) based on the volume and distribution of injured lung relative to the total lung volume.
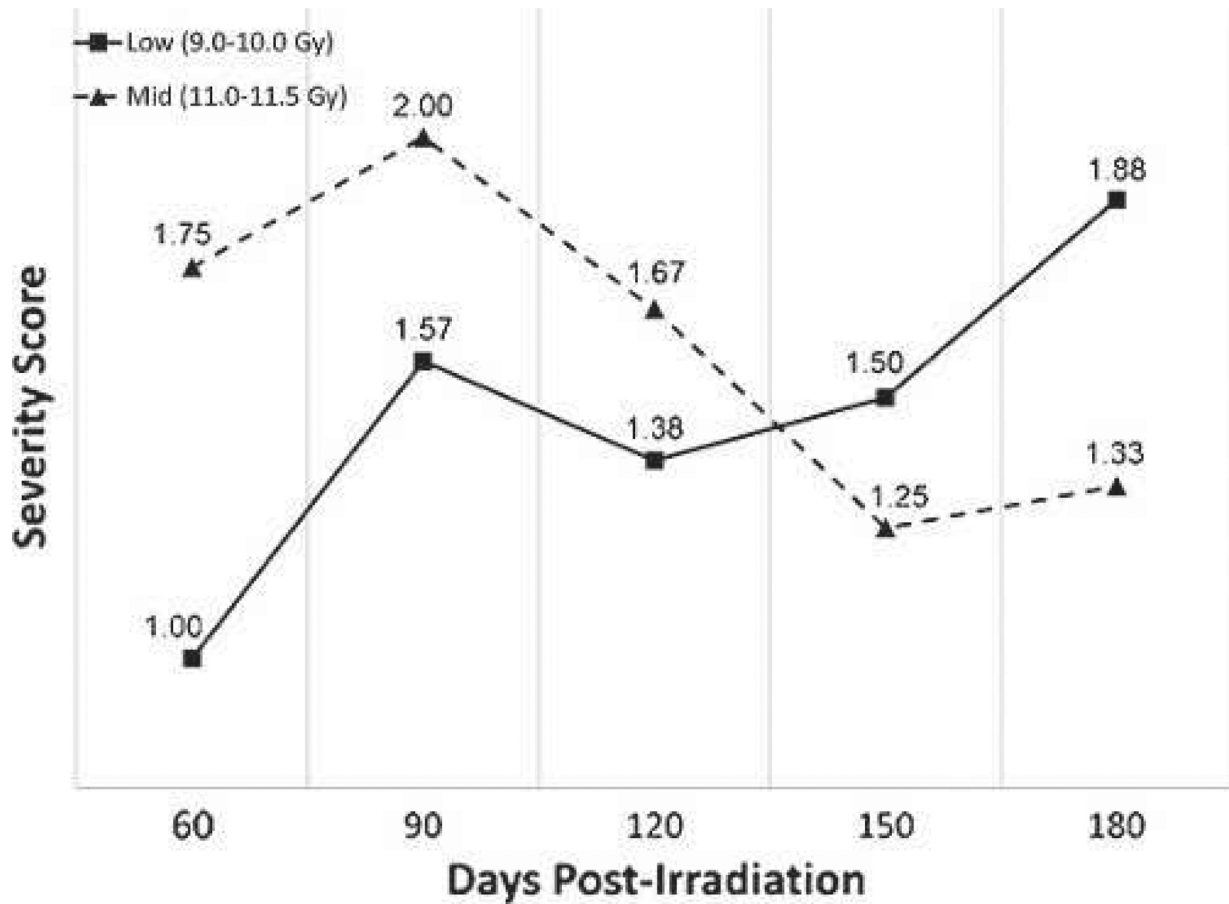
Fig. 13.
Time course of radiographic severity of pulmonary injury in rhesus macaques exposed to PBI/BM5. Serial, non-contrast enhanced, high-resolution CT scans were obtained in rhesus macaques approximately every 30 d post-irradiation. This analysis was restricted to NHPs that survived >60 d post-exposure (e.g., survivors of GI-ARS and H-ARS coincident with prolonged GI; $n = 28$) and for whom CT data were available ($n = 24/28$). Mean values are plotted for NHPs grouped into dose cohorts. Animals in the High (12.0–12.5 Gy) dose cohort are not shown, as only two of those NHPs survived >60 d, neither of which had serial CT data.
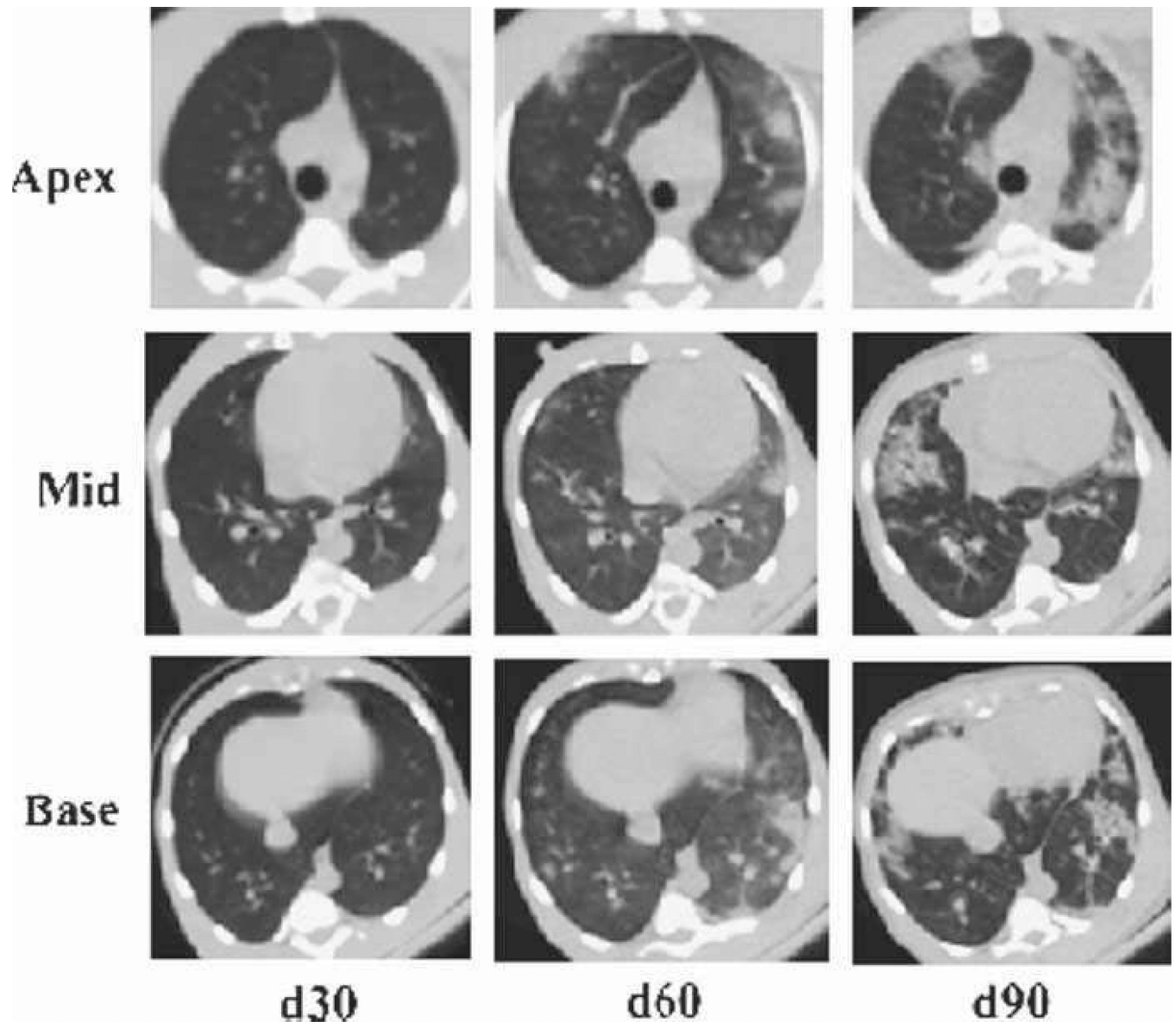
Fig. 14.
Evolution of radiographic injury in rhesus macaques exposed to PBI/BM5. Representative example of evolving radiation-induced pulmonary injury in a rhesus macaque post-11.0 Gy PBI/BM5. Images from the apex, mid, and base of the lung are shown at 30, 60, and 90 d post-exposure. This NHP was subsequently treated with dexamethasone (day 115 post-exposure) but succumbed to lung injury within 1 wk of beginning the corticosteroid treatment.
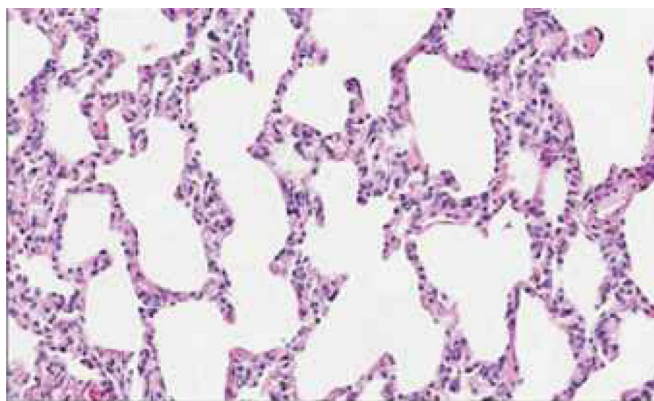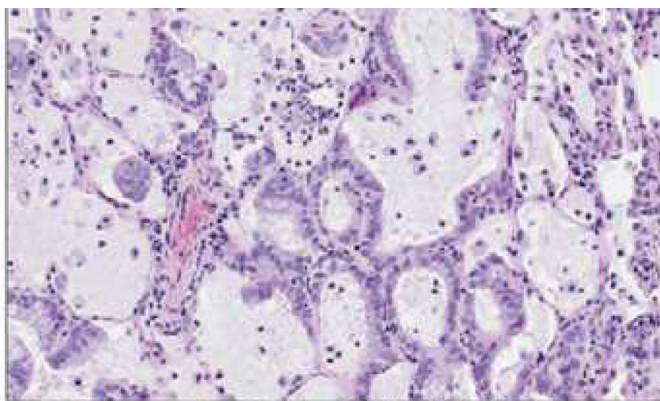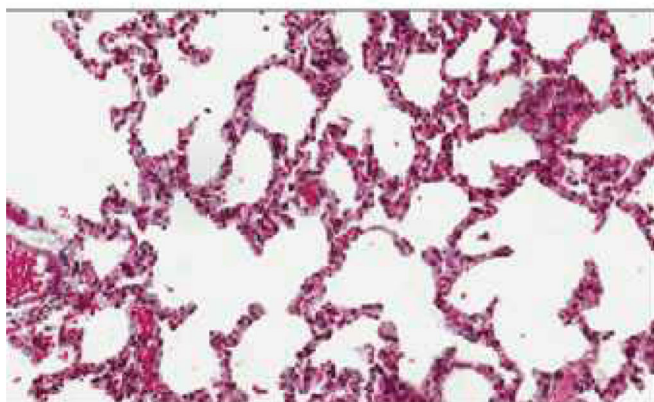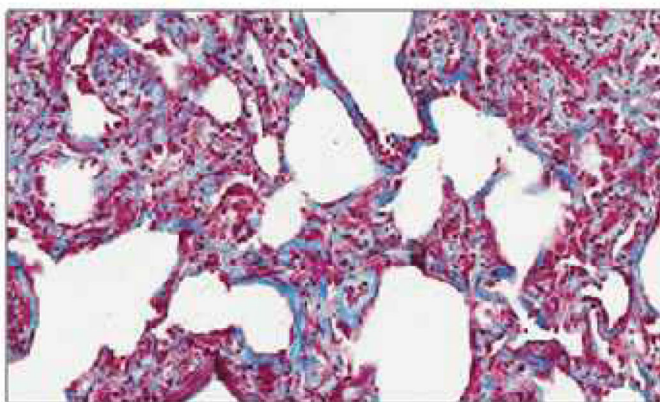
Fig. 15.
Histopathologic changes in the lungs of rhesus macaques exposed to PBI/BM5. Samples from normal (non-irradiated) NHPs are shown on the left, and samples from an NHP euthanized at day 182 post-10.0 Gy PBI/BM5 are shown on the right. H&E staining of the post-irradiation samples demonstrated macrophage infiltration with foamy macrophages, alveolar wall thickening, distortion of alveolar architecture, and hyaline membranes in the alveolar airspaces. Masson's trichrome staining demonstrated collagen deposition indicative of evolving fibrosis in the post-irradiation samples.

Table 1

The dose response relationship (DRR) for partial-body, total-body, and whole thorax lung irradiation of rhesus macaques. NHPs were exposed to 6 MV LINAC-derived photons at a dose rate of 0.80 Gy min⁻¹. All exposures are measured as midline tissue dose. The DRRs are defined by survival at 15, 60, and 180 d post- irradiation after exposure to a range of doses: PBI/BM5 animals were exposed in six dose cohorts of 9.0, 10.0, 11.0, 11.5, 12.0, and 12.5 Gy; TBI 60-d study animals were exposed in seven dose cohorts to 7.2, 7.50, 7.55, 7.85, 8.05, 8.40, 8.90 Gy (n = 110); TBI 15-d study animals were exposed to in eight dose cohorts to 10.0, 10.5, 11.0, 11.5, 12.0, 12.5, 13.0, and 14.0 Gy (n = 61); WTLI. The respective values are presented for LD10, LD50, LD90, slope, and total number of animals used in determining the DRR. The values for the DRR are derived from linear (no dose transform) normal probit fits. LD values are given with 95% confidence intervals in brackets.

Study	LD10(Gy)	LD50(Gy)	LD90(Gy)	Probit Slope	n
TBI 15 d	9.93[8.47,10.54]	11.33[10.81,11.75]	12.73[12.21,13.9]	0.92[0.49,1.34]	61
TBI 60 d	6.23[3.52,6.82]	7.45[6.94,7.69]	8.68[8.23,10.69]	1.05[0.36,1.74]	110
PBI 15 d	10.88[10.02,11.23]	11.95[11.64,12.51]	13.02[12.47,14.58]	1.20[0.58,1.81]	79
PBI 60 d	9.53[8.21,10.10]	11.01[10.57,11.41]	12.48[11.95,13.70]	0.87[0.48,1.25]	72
PBI 180 d	8.61[6.82,9.28]	9.73[8.91,10.17]	10.85[10.42,11.63]	1.14[0.58,1.71]	64
WTLI 180 d	9.16[8.18,9.60]	10.28[9.91,10.67]	11.41[10.95,12.42]	1.14[0.64,1.64]	58

Table 2

Percent lethality and survival time of decedents in rhesus macaques exposed to PBI/BM5. Doses were grouped into High (12.0–12.5 Gy), Mid (11.0–11.5 Gy), and Low (9.0–10.0 Gy) dose cohorts for analysis. Lethality is here defined by euthanasia or expiration before the endpoint of each sub-syndrome (15 d for G-ARS, 60 d for H-ARS, and 180 d for DEARE. Lethality is given as a percentage, followed by the raw number of animals (decedents/total) in parenthesis. Survival time (days) of decedents is given as the mean ± SEM.

| Dose cohort (Gy) | Lethality (%) | | |
	Days 0–15	Days 0–60	Days 0–180
Low (9.0–10.0)	6 (1/16)	25 (4/16)	44 (7/16)
Mid (11.0–11.5)	11 (3/27)	48 (13/27)	93 (25/27)
High (12.0–12.5)	71 (15/21)	90 (19/21)	100 (21/21)
Survival time of decedents	9.5 ± 0.6	17.6 ± 1.9	50.8 ± 7.3

Table 3

The onset and severity of dehydration in rhesus macaques exposed to PBI/BM5. The first day that moderate or severe dehydration was observed post-irradiation and the incidence of severe dehydration are given for (a) NHPs grouped into dose cohorts and (b) all studied NHPs, survivors, and decedents. Each animal's hydration status was assessed daily. First day values are means ± SEM. Incidence percentages are given with the number of affected NHPs over the total number of NHPs in the cohort in parenthesis.

a.

Dose cohort (Gy)	1st day of moderate or severe dehydration	% of cohort that became severely dehydrated
Low (9.0–10.0)	5.6 ± 0.6	25 (4/16)
Mid (11.0–11.5)	5.9 ± 0.3	41 (11/27)
High (12.0–12.5)	5.5 ± 0.2	76 (16/21)

b.

9.0–12.5 Gy	1st day of moderate or severe dehydration	% of cohort that became severely dehydrated
All animals	5.7 ± 0.2	48 (31/64)
Survivors	5.0 ± 0.5	9 (1/11)
Decedents	5.8 ± 0.2	57 (30/53)

Table 4

The onset and severity of weight loss in rhesus macaques exposed to PBI/BM5. The first day 10% of pre-TBI body weight loss was observed, and the greatest and least percentages of weight loss for an individual animal are given for (a) NHPs grouped into dose cohorts and (b) all studied NHPs, survivors, and decedents. Animals were weighed daily. First day values are means ± SEM.

a.

Dose cohort (Gy)	Incidence of weight loss 10% (%)	First day to 10% weight loss	Greatest loss (%)	Least loss (%)
Low (9.0–10.0)	75 (12/16)	8.9 ± 1.2	27.1	1.7
Mid (11.0–11.5)	100 (27/27)	10.2 ± 1.2	29.7	11.7
High (12.0–12.5)	100 (21/21)	6.9 ± 0.4	27.4	9.2

b.

9.0–12.5 Gy	Incidence of weight loss 10% (%)	First day to 10% weight loss	Greatest loss (%)	Least loss (%)
All animals	92 (59/64)	8.8 ± 0.6	29.7	1.7
Survivors	64 (7/11)	9.3 ± 1.7	25.0	1.7
Decedents	98 (54/55)	8.8 ± 0.7	29.7	9.2

Table 5

The onset and severity of diarrhea in rhesus macaques exposed to PBI/BM5. The first day that diarrhea was observed post-irradiation, the first day blood was observed in stool, and the incidence of bloody stool are given for (a) NHPs grouped into dose cohorts and (b) all studied NHPs, survivors, and decedents. Each animal's stool consistency was monitored twice a day for the duration of the in vivo phase of the study. The presence of blood in stool was evaluated concurrently. First day values are means ± SEM. Incidence percentages are given with the number of affected NHPs over total number of NHPs per cohort in parenthesis.

a.

Dose cohort (Gy)	First day of diarrhea	First day of blood in stool	% of cohort that experienced blood in stool
Low (9.0–10.0)	4.2 ± 0.4	8.3 ± 0.9	75 (12/16)
Mid (11.0–11.5)	4.6 ± 0.2	12.9 ± 1.8	85 (23/27)
High (12.0–12.5)	4.0 ± 0.5	8.1 ± 0.8	76 (16/21)

b.

9.0–12.5 Gy	First day of diarrhea	First day of blood in stool	% of cohort that experienced blood in stool
All animals	4.3 ± 0.2	10.3 ± 0.9	65 (51/64)
Survivors	4.0 ± 0.4	8.1 ± 1.4	64 (7/11)
Decedents	4.4 ± 0.2	10.6 ± 0.9	83 (44/53)

Table 6

The incidence and onset of neutropenia in rhesus macaques exposed to PBI/BM5. The incidence of grade 3 and 4 neutropenia, the first day each grade was observed post-irradiation, and the duration of each grade is given for NHPs grouped into dose cohorts. Neutropenia grades were defined as ANC 500 μL^{-1} for grade 3 and ANC 100 μL^{-1} for grade 4. Recovery is defined as two consecutive days with ANC 1,000 μL^{-1}. CBC and manual WBC differentials were performed daily for each animal. First day values are means ± SEM. Incidence percentages are given with the number of affected NHPs over the total number of NHPs in the cohort given in parenthesis.

Dose cohort (Gy)	Incidence of neutropenia (%)		First day of neutropenia		Incidence of recovery (%)	First day of recovery
	Grade 3	Grade 4	Grade 3	Grade 4		
Low (9.0–10.0)	94 (15/16)	56 (9/16)	4.6 ± 0.3	6.0 ± 0.4	87 (13/15)	25.6 ± 1.0
Mid (11.0–11.5)	100 (27/27)	63 (17/27)	4.7 ± 0.1	6.8 ± 0.5	63 (17/27)	24.8 ± 2.5
High (12.0–12.5)	100 (21/21)	62 (13/21)	4.4 ± 0.1	5.6 ± 0.3	24 (5/21)	18.6 ± 2.9
All animals	98 (63/64)	61 (39/64)	4.6 ± 0.1	6.2 ± 0.3	56 (35/64)	24.2 ± 1.4

Table 7

The incidence and onset of febrile neutropenia and infection in rhesus macaques exposed to PBI/BM5. The incidence and first day of febrile neutropenia post-irradiation, and the incidence of positive blood cultures is given for NHPs grouped into dose cohorts. Febrile neutropenia was defined as ANC   500 μL^{-1} with body temperature   103.0 °F. CBCs, and manual WBC differentials were performed daily for each animal. Blood cultures were collected upon observation of febrile neutropenia. First day values are means ± SEM. Incidence percentages are given with the number of affected NHPs over the total number of NHPs in the cohort given in parenthesis.

Dose cohort (Gy)	Incidence of febrile neutropenia (%)	First day of febrile neutropenia	Incidence of positive blood culture (%)
Low (9.0–10.0)	56 (9/16)	13.6 ± 2.5	25 (4/16)
Mid (11.0–11.5)	33 (9/27)	15.9 ± 2.4	19 (5/27)
High (12.0–12.5)	5 (1/21)	8.0	5 (1/21)
All animals	30 (19/64)	14.4 ± 1.7	16 (10/64)

Table 8

The incidence and onset of thrombocytopenia in rhesus macaques exposed to PBI/BM5. The incidence, first day, and duration of thrombocytopenia observed post-irradiation, and the incidence of first day of whole blood transfusion is given for NHPs grouped into dose cohorts. Thrombocytopenia is defined as platelets < 20,000 μl^{-1}. CBCs were performed daily for each animal. First day values are means ± SEM. Incidence percentages are given with the number of affected NHPs over the total number of NHPs in the cohort given in parenthesis.

Dose cohort (Gy)	Incidence of thrombocytopenia (%)	First day of thrombocytopenia	Duration of thrombocytopenia	Incidence of transfusions (%)	First day of transfusion
Low (9.0–10.0)	75 (12/16)	9.3 ± 0.4	7.4 ± 1.5	19 (3/16)	10.7 ± 1.2
Mid (11.0–11.5)	81 (22/27)	9.6 ± 0.2	10.7 ± 2.3	37 (10/27)	12.0 ± 0.5
High (12.0–12.5)	62 (13/21)	8.6 ± 0.3	8.3 ± 1.9	24 (5/21)	11.4 ± 1.0
All animals	73 (47/64)	9.3 ± 0.2	9.4 ± 1.4	28 (18/64)	11.6 ± 0.4

Table 9

Incidence and latency of pneumonitis in rhesus macaques exposed to PBI/BM5. Incidence of and latency to development of clinical pneumonitis in rhesus macaques [defined as developing a non-sedated respiratory rate (NSRR) > 80] post-irradiation. This analysis was restricted to NHPs who survived GI-ARS and H-ARS coincident with prolonged GI damage (e.g., >60 d post-exposure; $n = 28$) and for whom serial daily NSRR data were available ($n = 15/28$). Mean latency to development of pneumonitis is shown ± SEM. Survival rates and mean survival times for NHPs living at least 60 d are shown ± SEM.

Radiation dose (Gy)	Incidence of clinical pneumonitis	Mean latency to clinical pneumonitis ± SEM (d)	Survival rate for NHPs surviving at least 60 d	Mean survival time of day 60+ decedents ± SEM (d)
9.0	40.0% (2/5)	101.0 ± 0	100% (5/5)	N/A
10.0	50.0% (1/2)	97.0 ± 0	42.9% (3/7)	143.5 ± 18.5
Low	**42.9% (3/7)**	**99.7 ± 1.33**	**66.7% (8/12)**	**143.5 ± 18.5**
11.0	60.0% (3/5)	102.0 ± 12.1	22.2% (2/9)	134.9 ± 11.1
11.5	33.3% (1/3)	93 ± 0	0% (0/5)	108.2 ± 16.9
Mid	**50.0% (4/8)**	**99.8 ± 10.9**	**14.3% (2/14)**	**123.8 ± 9.9**
12.0	N/A	N/A	0% (0/2)	91.5 ± 10.5
12.5	N/A	N/A	N/A	N/A
High	**N/A**	**N/A**	**0% (0/2)**	**91.5 ± 10.5**

Table 10

Radiographic incidence of pulmonary injury in rhesus macaques exposed to PBI/BM5. Serial, non-contrast enhanced, high-resolution CT scans were obtained in rhesus macaques approximately every 30 d post-irradiation. This analysis was restricted to NHPs that survived >60 d post-exposure (e.g., survivors of GI-ARS and H-ARS coincident with prolonged GI; $n = 28$) and for whom CT data were available ($n = 24/28$). Incidence was calculated for each time point at which CT scans were taken.

Radiation dose (Gy)	d30/45	d60	d90	d120	d150	d180
9.0	0% (0/5)	40% (2/5)	60% (3/5)	80% (4/5)	60% (3/5)	60% (3/5)
10.0	0% (0/2)	25% (1/4)	66.7% (4/6)	66.7% (4/6)	100% (5/5)	100% (5/5)
Low	**0% (0/9)**	**33.3% (3/9)**	**63.6% (7/11)**	**72.7% (8/11)**	**80% (8/10)**	**80% (8/10)**
11.0	0% (0/4)	83.3% (5/6)	100% (6/6)	100% (5/5)	100% (3/3)	100% (3/3)
11.5	0% (0/4)	75% (3/4)	100% (2/2)	100% (1/1)	100% (1/1)	N/A
Mid	**0% (0/8)**	**80% (8/10)**	**100% (8/8)**	**100% (6/6)**	**100% (4/4)**	**100% (3/3)**
12.0	0% (0/1)	100% (1/1)	N/A	N/A	N/A	N/A
12.5	N/A	N/A	N/A	N/A	N/A	N/A
High	**0% (0/1)**	**100% (1/1)**	N/A	N/A	N/A	N/A